# The Mass Loss Mechanisms of Polymers in a Radio Frequency Induced Atomic Oxygen Environment

A. F. WHITAKER[1] and B. Z. JANG*[,2]

[1]NASA Marshall Space Flight Center, EH 11, Huntsville, Alabama 35812, and [2]Materials Engineering Program, Composites Research Labs, 201 Ross Hall, Auburn University, Alabama 36849

**SYNOPSIS**

The effects of atomic oxygen on several classes of polymers were investigated. Particular attention was directed to the determination of erosion or mass loss mechanisms in relation to the physical and chemical structures of polymers. Nineteen polymeric materials were exposed to a thermal atomic oxygen environment at fluxes of $10^{22}$ atoms/$m^2$-sec. Bulk material temperatures were maintained at 10, 45, and 75°C during exposure. Mass loss rate, which was characteristic of the type of polymer, was proportional to the exposure area and was linear in time for most polymers except for Mylar, which produced a shielding high temperature ash. The mass loss rate for the atomic oxygen degradation of polymers was related to the bond strength of the polymer structure and to the shielding effect of pendant structures. This degradation process was strongly dependent on polymer temperature. Activation energies ranged from 1 to 48 KJ/mole and were found to be related to gaseous diffusion in polymers. Frequency factors were proportional to activation energies. Activation energies were found to increase with increased mol wt and crosslinking. An equation was developed relating exposure area, atomic oxygen flux, frequency factor, and activation energy to the rate of polymer mass loss. © 1993 John Wiley & Sons, Inc.

## INTRODUCTION

Polymer films have been increasingly used in space missions. For instance, the films are utilized in spacecraft to maintain thermal control or to serve as structural substrates for solar arrays. Since these materials are subject to atomic oxygen attack, it is important to understand the nature of this attack on materials. Ground-based studies of atomic oxygen effects on materials generally involved the utilization of oxygen gas plasma that was activated by a radio frequency.[1]

Atomic oxygen, along with other plasma activated gas species, is utilized to condition polymer surfaces for improved bonding.[2-6] The majority of the research related to this process occurred in the 50s, 60s, and early 70s. There are several categories of gas–polymer surface interactions: absorption of the gas, removal of a weak surface layer by oxidation, cleaning of the surface by removal of adsorbed materials through kinetic action, crosslinking of the surface, and chemical reactions, including the introduction of polar groups, such as ketones, hydroxyl, ether, peroxides, and carboxylic acid groups. The surfaces of some polymers, such as polycarbonate, polypropylene, and polyethylene, have shown no indication of crosslinking, as evidenced by their failure, after exposure to an oxygen plasma, to produce a gel.[7] Yasuda et al.[8] concluded that crosslinking by the plasma was negligible unless the polymer had low plasma susceptibility and/or high capability to crosslink. Klein and Scheer[9] studied the addition of atomic oxygen to condensed olefin films and observed that the olefin films behaved as a sink for atomic oxygen atoms over a wide range of olefin concentrations, and suggested that the oxygen atoms, once incorporated into the film, diffuse freely until they react with an olefin molecule. Rossmann,[10] in his bonding studies of polyethylene using a glow discharge, concluded from IR data generated on treated polyethylene that the improvement of bonding properties was accompanied by dehydro-

* To whom correspondence should be addressed.

Journal of Applied Polymer Science, Vol. 48, 1341–1367 (1993)
 CCC 0021-8995/93/081341-27

genation and subsequent partial oxidation of the polyethylene molecule.

Hansen et al.[11] presented the first mass loss rate data on polymers exposed to atomic oxygen produced by a radio frequency (R–F) discharge. Test pressures were 1 mm Hg, with atomic oxygen concentration estimated as $10^{14}$–$10^{15}$ atoms/cc and temperature believed to be less than 70°C. A mass loss rate for each of 36 polymers was generated. All polymers reacted, but the more highly branched polymers were more readily attacked. Gas spectra showed evidence of strong $CO_2$ and OH bands for hydrocarbon polymers, such as polyethylene. Antioxidents appeared to have no effect on the magnitude of mass loss rate. Mass loss was immediate upon exposure with no induction period as is usually seen in photo or thermal oxidation.[12,13] Hansen et al.[11] proposed that atomic oxygen behaved as a radical and initiated oxidation of hydrocarbons by the rapid reaction, as given by eq. (1) below.

$$XH + O \xrightarrow{\text{rapid}} X' + X''O \text{ or } X + OH \qquad (1)$$

This reaction then would be followed by a rapid reaction of the product radical with atomic oxygen, eq. (2).

$$X + O \xrightarrow{\text{rapid}} XO \qquad (2)$$

Hansen et al. further determined that irradiation by electrons resulted in acceleration of mass loss rates. In some cases, it was surmised that during oxidation, simple ablation of the polymer surface occurred because the polymer surface oxidized and volatilized. MacCallum and Rankin[14] exposed five hydrocarbon polymers to atomic oxygen. Mass spectrometry of volatile products revealed only carbon dioxide and water vapor. Examination of residual films by IR and UV spectroscopy revealed no chemical changes to have taken place. Taylor and Wolf[15] reported removal rates for 33 polymers, which were spun coated on silicon wafers and then exposed for 2 min to an oxygen plasma. While exposed to the oxygen plasma, the wafers were placed on a plasma preheated aluminum table, which Taylor and Wolf claimed to have stabilized at 35°C. Among their conclusions were that strong polymer backbone and backbone–side chain bonds confer stability to atomic oxygen, whereas weak backbone–side chain bonds afford enhanced degradation. They showed that the removal rate of poly(2,3-dichloro-1-propyl acrylate) and poly(*N*-vinylcarbazole) are temperature sensitive. They suggested that the rate-determining step may have been cleavage of the backbone bonds, but that it was not apparent for crosslinking polymers. Further, they attributed the resistive nature of the polydimethyl silicones to the formation of a thin, protective ~ 100 Å layer of $SiO_2$. Several investigators[16,17] have confirmed this finding.

Moss et al.,[18] in an effort to gain a better understanding of the stripping process of plasma developable photoresists, studied the effects of an oxygen plasma on the copolymers of methyl methacrylate, styrene, and vinyl naphthalene. No attempt was made to control substrate temperatures during these tests. Several stages to polymer/oxygen plasma interactions were suggested. These proposed stages consisted of radical site formation on the polymer followed by further reactions with the oxygen plasma. In addition, their studies suggested that the benzene ring-containing structures are more stable as a result of the formation of phenols on the ring, which block the initiation stage of plasma oxidation. Moss et al. tentatively suggested that the low etch rate of the glycidyl methacrylate homopolymer is a function of its relatively high degree of crosslinking rather than the primary structure of the parent polymer repeat unit.

Torre and Pippin[19] extended the idea, concerning polymer resistance to atomic oxygen attack, through the interpretation of existing data and Boeing in-house measurements. Structures containing stronger bonds exhibited more resistance to attack than structures with weaker bonds. Side groups tended to shield atomic oxygen from attacking the backbone. Fluoridation of the ethylene structure decreased the mass loss rate relative to polyethylene. They suggested that recombination of oxygen atoms on the surface was energetic enough to break many types of bonds and could explain on-orbit mass loss as well as collisional processes. Arnold and Peplinski[20] suggested, from their studies of Kapton using a DC arc-heated atomic oxygen beam source, that the reaction rate had little dependence on relative collision energies within the range of 1–5 eV.

The purpose of this investigation was to obtain a quantifiable understanding of the nature of atomic oxygen attack on polymeric materials. This understanding is necessary in order to select structural films or develop protective coatings for spacecraft surfaces that will have increased durability under atomic oxygen exposure. As a first step, an effort was made to characterize the nature of an oxygen plasma induced by radio frequency.[1] Relative concentrations of various charged and neutral particles were determined. With a plasma pressure range of 500 to 900 millitorr at 40 and 60 watts input power, the electron temperature was found to increase

slightly both with pressure and input power, while the electron concentration remained essentially constant at approximately $4.4 \times 10^{14}$ $m^{-3}$ over this same pressure and power range. Under the same conditions, the concentration of atomic oxygen atoms ranged from 0.91 to $1.87 \times 10^{20}$, which represented 1% or less of the total pressure. The ions and electrons in the plasma were found to contribute little to the mass loss of polymers. The effect of sputtering on the mass loss rate of polymers was also insignificant. Mass loss of polymers in the oxygen plasma environment was primarily caused by the atomic oxygen.

With these considerations in mind, this study of several polymeric materials was undertaken with the following objectives: (1) Determination of the relationship of material structure to mass loss as a result of atomic oxygen exposure; (2) determination of the role of temperature in the atomic oxygen attack of these polymeric materials; (3) determination of whether or not a relationship exists between mol wt and atomic oxygen effects on selected polymeric materials.

## EXPERIMENTAL

### Polymer Mass Loss Determination

Polymer mass loss rate was determined via the test system described earlier.[1] This test system would allow a unit surface area of this film polymer to be exposed to the oxygen plasma for selected durations. Specimens could be exposed for several hours while the bulk material was maintained at a selected constant temperature. The specimens were removed periodically from the plasma exposure to be weighed for mass loss rate determinations.

The plasma reaction unit ("Plasmod" from Tegal Corporation) consisted of a RF generator, a vacuum pump, associated valving, and a Pyrex glass reaction chamber. The RF source could provide up to 100 watts of continuous 13.56 MHz power to the reaction chamber. The RF energy was used to dissociate the molecular oxygen into an oxygen plasma. The reaction chamber, which was modified for these investigations, consisted of a Pyrex glass chamber, a silicone gasket vacuum seal, and a coated Plexiglas door, which holds the material test plate. The material test plate consisted of a copper block base, a thermoelectric module, a material test sample, a glass cover plate, and a thermocouple. The details of this plasma reaction chamber have been specified earlier.[1]

### Residual Gas Analyses

Residual gas analyses (RGA) of the gases in the Plasmod chamber during material exposure were undertaken in order to provide additional insight into the erosion of the polymer under atomic oxygen attack. Analyses of residual gases, generated from the oxygen plasma-exposed materials, were measured using a UTI Model Quadruple Mass Analyzer. The RGA system was composed of the mass spectrometer with an associated vacuum pumping system. This system was placed adjacent to the Plasmod during testing and a stainless steel tube was routed from the RGA system through a specially configured Plexiglas door for this testing. On the Plasmod interior side to the Plexiglas door, the tube was glass and it extended approximately to the surface of the suspended material specimen in order to sample the evolved gasses as the material was exposed. Since the Plasmod was not operated as a high vacuum chamber, the mass spectrometer could not directly receive the evolved gases. The gases were pumped into the intermediate pressure chamber of the analyzer system. This allowed the gas pressure to be reduced from 800 millitorr to approximately 8000 nanotorr so that gas analyses by the mass analyzer could be accomplished.

### Characterization of the Oxygen Plasma

Since a plasma is an electrically neutral gas, but contains a collection of ions, electrons, and neutral atoms, it is necessary to characterize separately the charged particles and the neutral gases. The approach to this characterization was to use an electrostatic probe[31] for the charged particles and a catalytic surface[32] for the neutral atoms. This has been accomplished earlier.[1]

### Materials and Sample Preparation

Nineteen polymeric systems, representing various bond strength configurations, which are of interest to the space program, were selected for the present study. These included polyethylene (three mol wts), polymethyl methacrylate (two mol wts), PMMA (two mol wts), polyethylene terephthalate, polyimide, polytetrafluorethylene (PTFE), perfluorinated ethylene propylene copolymer (FEP), polypropylene (PP), and polyvinyl fluoride (PVF).

Several methods were utilized to prepare films from the powders supplied by the National Bureau of Standards. Films of PE, PS, and PMMA were prepared by: (1) vacuum evaporation on a Teflon

sheet from a spectral grade acetone solution, (2) melting and solidification in air on a Teflon sheet, and (3) hydrostatic pressing. These films varied in thickness and surface morphology. Consequently, differences were encountered in their mass loss rate determination, and morphological surface features, present in materials prior to oxygen plasma exposure, interfered with any characterization of surface features produced by the plasma. Films were cleaned with high purity acetone or ethanol, depending on compatibility, followed by distilled water wash. They were air dried and vacuum dried prior to weighing and plasma exposure.

### Analyses of Polymers and Polymer–Atomic Oxygen Interactions

Polymeric films, including thermosetts and thermoplastics, configured for constant projected area exposure and maintained at constant bulk temperatures were subjected to a characterized active oxygen plasma. Mass loss was measured as a function of time and temperature. The time and temperature of exposure was set according to the reactivity and upper use temperature of the polymer and test system constraints. An activation energy of the temperature dependence of the atomic oxygen erosion process of materials under nominal operating plasma conditions was derived.

Techniques, utilized to assist in the analyses of the materials and their interactions with atomic oxygen, included:

| Technique | Rationale for Use |
|---|---|
| Residual gas analysis | Gaseous products, evolved from materials, were determined during exposure for five polymers. |
| Scanning Electron Microscopy (SEM) | Observation and comparison of surface structures of polymer surface morphology was accomplished by this analysis. |
| Fourier Transformation Infrared (FTIR) | This was highly sensitive analyses of polymer structures. By utilizing thin specimens, surface residue contributions to structure should have been visible. Chemical changes, due to atomic oxygen, would be noted through this technique in combination with ESCA analyses. |
| Electron Spectroscopy for Chemical Analysis (ESCA) | These were sensitive surface analysis techniques. They should have yielded data on the surface residues. |
| Gel Permeation Chromatography (GPC) | This yielded mol wt analyses of polymers and was required for both exposed and unexposed polymers. It was intended to be used to indicate a change in surface mol wt as a result of AO exposure. |

The FTIR, ESCA, and part of the GPC was accomplished via contract. The effects of atomic oxygen on mol wt were studied using polyethylene, PS, and PMMA. Where possible, a comparison was made between flight data and laboratory data on these materials.

The environment of the oxygen plasma was characterized according to total particle density, density of ions, and electron temperature at various pressure, and R–F energy inputs. Selected polymers were exposed at constant temperature to show effects of RF energy input and pressure differences.

All materials were exposed to the oxygen plasma at a specified input energy and pressure at three different temperatures up to a maximum temperature of 90°C, where feasible. Exposure data for all test specimens was obtained over an area of approximately 0.4 $in^2$ ($2.84 \times 10^{-4}$ $m^2$).

## RESULTS AND DISCUSSION

### Mass Loss Data as a Function of Time and Temperature

Representative mass loss rate data are shown in Figures 1–3, while the data on other polymers investigated are given in Ref. 21. No mass loss could be detected for dimethyl silicone and NaCl. All polymers within experimental uncertainties were found to lose mass linearly with time over the test durations, with the exception of Mylar, whose rate decreased with time and polystyrene, which provided

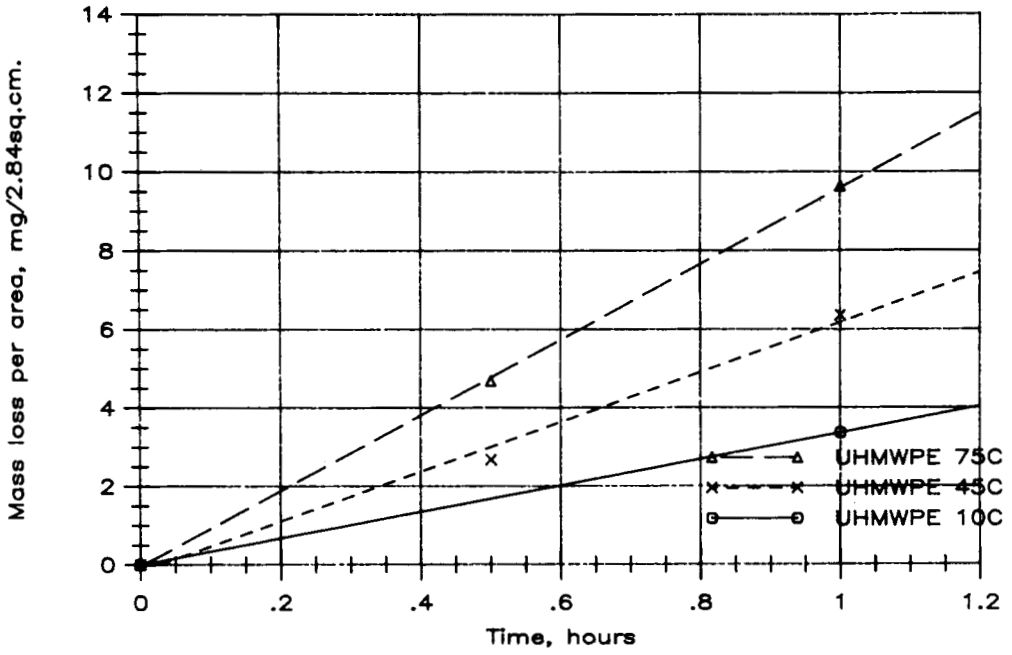


**Figure 1** Mass loss per area vs. time for UHMWPE.

mixed results. Visible ash was evident on the Mylar surface and appeared to accumulate during testing, thus providing some surface shielding. Mass loss rate was found to be directly related to the exposure area and to be independent of sample thickness, as has been reported by other investigators previously mentioned. Comparative mass loss data is presented in Table I. Some general observations are made relative to this data. These materials, which were thermally controlled, showed a different ranking for the

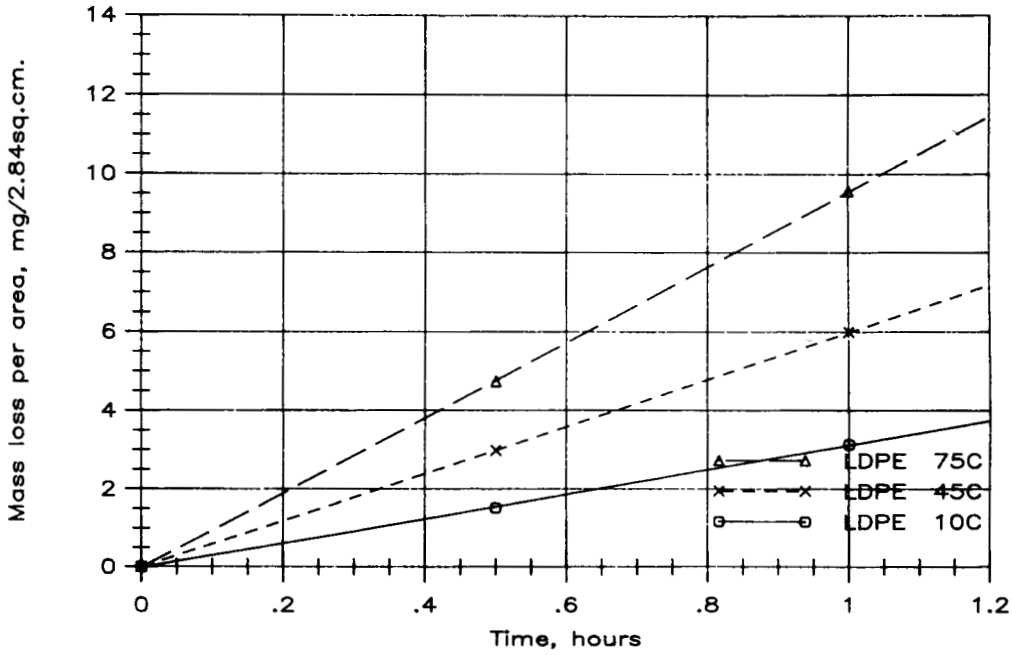


**Figure 2** Mass loss per area vs. time for LDPE.

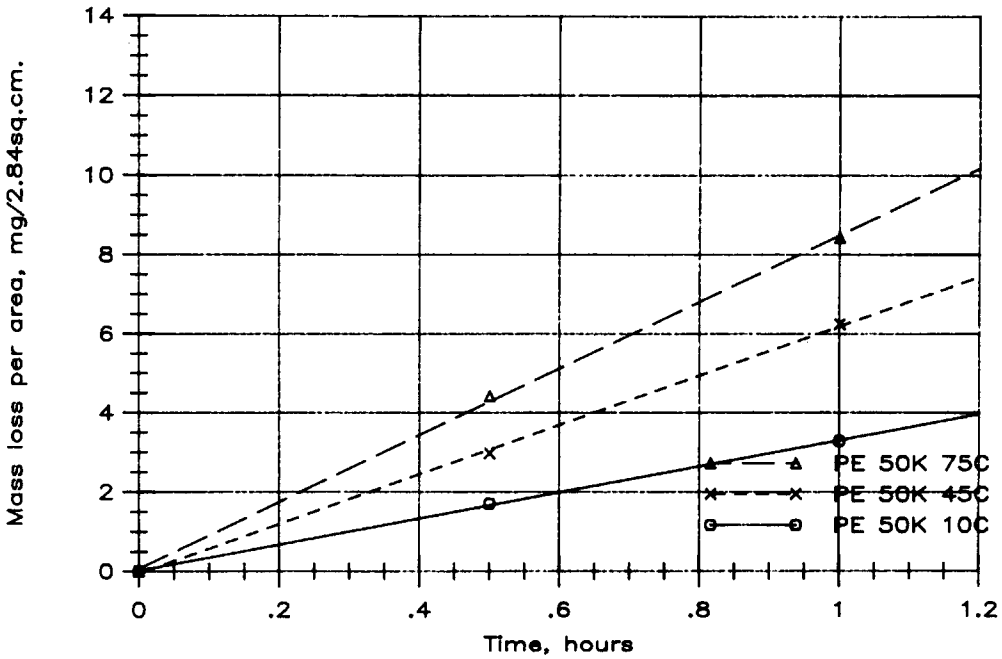


**Figure 3** Mass loss per area vs. time for PE 50 K.

same materials tested by Hansen et al.,[11] where the material temperature was uncontrolled. Comparison of mass loss for HDPE to that of LDPE showed essentially no differences, so that the trend of branched vs unbranched PE in this environment could not be distinguished based on mass loss rate alone. Other than the dimethyl silicones, the fluorinated polymers were more stable in this environment with the resistance to attack increasing with an increase in the degree of fluorination. However, the effect of a single attached fluorine to the backbone, per repeating unit, added little resistance to attack; this suggested that the fluorine atoms shielded the backbone structure from atomic oxygen attack. Torre and Pippin[19] also proposed that some side groups also shield against attack of the backbone structure.

Control of material temperature allowed confirmation that the atomic oxygen-induced mass loss is a thermally activated process. Activation energies were determined from the referenced data and representative plots of this data are shown in Figures 4–7. A summary of the activation energies are shown in Table II. These activation energy values are smaller by a greater order of magnitude than the covalent bond energies,[22] so that covalent bond rupture could not explain the source of these energy values. The lower AO energy values were determined for the fluorinated materials, while the larger energy values were derived for polymers such as polyamide, which have strong polar interchain attractions.[23] A trend toward an increase in activation energy with an increase in mol wt and crosslinking was observed.

## Mass Loss as a Function of Atomic Oxygen Flux

Atomic oxygen flux increased both with increased pressure and increased Plasmod operational voltage (Table III). This variation in AO flux was reflected in the mass loss data also shown for various polymers. As anticipated, mass loss was found to be directly proportional to atomic oxygen flux within experimental uncertainty.

## Theory of Mass Loss

Mass loss rate variation with temperature suggested that this phenomena obeyed an Arrhenius law of the form

$$dm/dt = ce^{-Ea/RT} \tag{1}$$

where $dm/dt$ is the mass loss rate, $c$ is a constant, $Ea$ is the thermal activation energy, $R$ is the gas constant and $T$ is the absolute temperature.

Since exposure area and flux contributed to the magnitude of $dm/dt$, they could be incorporated into eq. (1) through the following derivation. Mass loss per time per area was the experimental measured quantity. It could be described in general terms of

**Table I Material Mass Loss Rate**

| Polymer | Rate of Mass Loss $10^{-6}$ (kg/h/Area) |
|---|---|
| Dimethyl silicone | Indeterminate |
| NACL | Indeterminate |
| Polytetrafluoroethylene | 0.78 |
| Polyvinylidene fluoride | 0.80 |
| Fluorinated ethylene propylene caprolyner | 1.1 |
| Polystyrene | |
| 670 K | 1.5 |
| 2610 K | 2.0 |
| Kapton | 1.1 |
| @ $10^{13}$ $p^+$, 400 KeV | 1.0 |
| Polycarbonate | 2.7 |
| Epoxy 956 | |
| @ 6 ± 1 h cure | 3.5 |
| @ 24 ± 2 h cure | 4.1 |
| @ 48 ± 2 h cure | 3.2 |
| @ 72 ± 2 h cure | 3.8 |
| Mylar | 3.6 ± .5 |
| Epoxy 507 | |
| @ 6 ± 1 h | 4.3 |
| @ 24 ± 2 h | 4.4 |
| Polypropylene | 5.5 |
| Polyvinyl fluoride | 6.2 |
| Polyethylene | |
| UHMWPE | 6.3 |
| 119 K PE | 5.9 ± 2.0 |
| 50 K PE | 6.2 |
| HDPE | 6.2 |
| @ $10^{13}$ $p^+$, 400 KeV | 4.7 |
| LDPE | 6.0 |
| Nylon 6 | 7.2 |
| @ $10^{13}$ $p^+$, 400 KeV | 6.1 |
| PMMA[a] | |
| 300 K | 22.6 |
| 1400 K | 5.4 |

Note: Material bulk temperature 45°C; atomic oxygen flux $3.13 \times 10^{22}$ atoms/m$^2$/sec.
[a] Data at 25°C.

the observed phenomena occurring at the material surface. A certain flux of atomic oxygen (AO) atoms was incident on a prescribed area of material, which resulted in a specific mass loss. Mathematically, this can be expressed as

$$1/A\ dm/dt = \delta m/\delta\epsilon\ (1/A\delta n/\delta t)\ \delta\epsilon/\delta n$$

$$1/A\ dm/dt = \delta m/\delta\epsilon\ (1/4n_v v)\ \delta\epsilon/\delta n \qquad (2)$$

where $A$ is exposed area of material, $\delta m/\delta\epsilon$ is the mass loss per mass loss event, $n_v$ is the number of AO atoms per volume, $v$ is the average velocity of the AO atoms, and $\delta\epsilon/\delta n$ is the number of mass loss events per incident AO atom. Now $\delta\epsilon/\delta n$ can be expressed as

$$\delta\epsilon/\delta n = \phi e^{-Ea/RT} = \tau \qquad (3)$$

where $\phi$ is a constant. $\delta\epsilon/\delta n$, hereafter to be referred to as $\tau$, is the mass loss probability or the mass loss event per atom impacting the polymer surface. Included in the value of $n$ are the surface reflected and recombined atoms. If eq. (3) is substituted into eq. (2), the mass loss rate equation then becomes

$$1/A\ dm/dt = \delta m/\delta\epsilon\ (1/4n_v v)\ \phi e^{-Ea/RT} \qquad (4)$$

The average magnitude of $\delta m/\delta\epsilon$ was estimated from the kinetic studies of AO exposed molecules, which were representative of the constituents of the solid polymer molecules of interest here.[24,25] Further, residual gas analysis (RGA) of the plasma gases to be discussed was undertaken to contribute to this analysis. Finally, the only unknown term of eq. (4) was $\phi$, which can be determined by substitution of the other quantities. The parameters of this equation for the various materials are presented in Table IV. These data are the values of the parameters in the equation, $\tau = \phi e^{-Ea/RT}$, for the various test temperatures.

The activation energies determined were considerably less than covalent bond energies and macroradical recombination energies.[26] A comparison of activation energies for gaseous diffusion in polymers[27-30] is shown in Table V, along with the AO reaction activation energies. As noted, these energies are the same magnitude and suggest that the AO generated energy is an activation energy for diffusion of atomic oxygen. The oxygen atom diameter is estimated to be about 1.40 Å,[31] which makes it one of the smaller gas diameters. As expected, since the activation energy for diffusion tended to increase with the increased diameter of diffusing atom,[32] energy values for atomic oxygen diffusion were lower than those for $O_2$ and $N_2$ in the same polymer.

Free volume in the polymer determined the ease or difficulty of diffusant atom transport.[33-35] Meissner[36] has described the temperature dependence of electrical conductivity by a generalized, free-volume equation, in which the temperature coefficient of fractional free volume was allowed to assume different values above and below the glass transition temperature ($T_g$). This extended the free

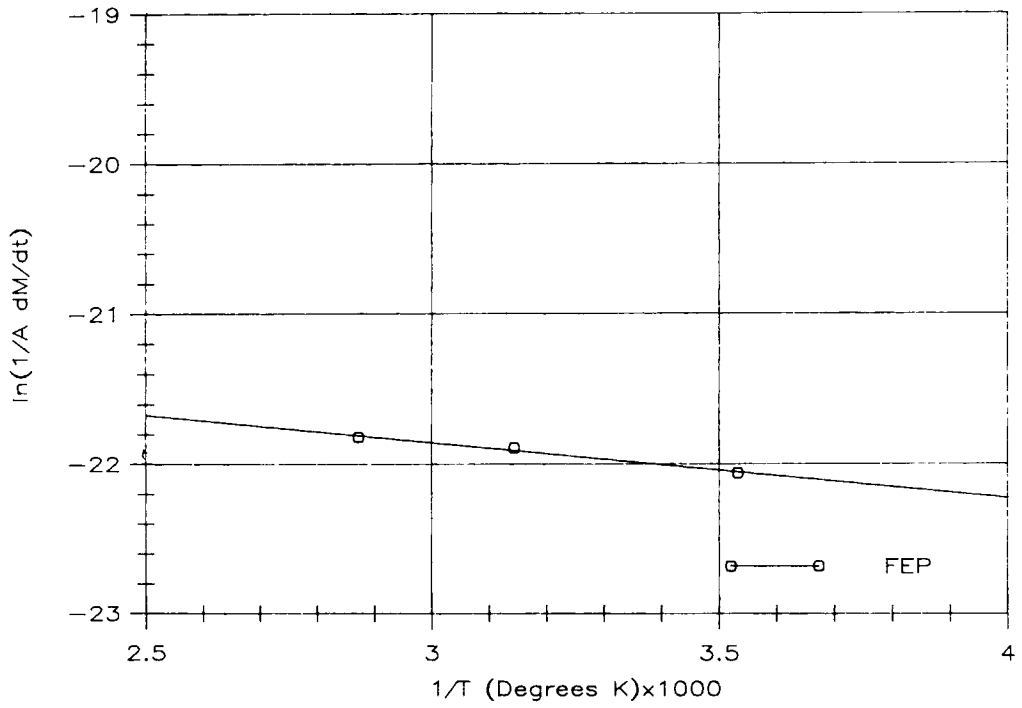


**Figure 4** Log (mass loss per area) vs. 1/T for FEP.

volume concept to sub-$T_g$ temperatures and assumed that molecular mobility was controlled by the available free volume in the glassy region, as well as in the melt region. The authors have chosen to represent the customary fractional free volume equation,

$$f = fo + b(T - To) \qquad (5)$$

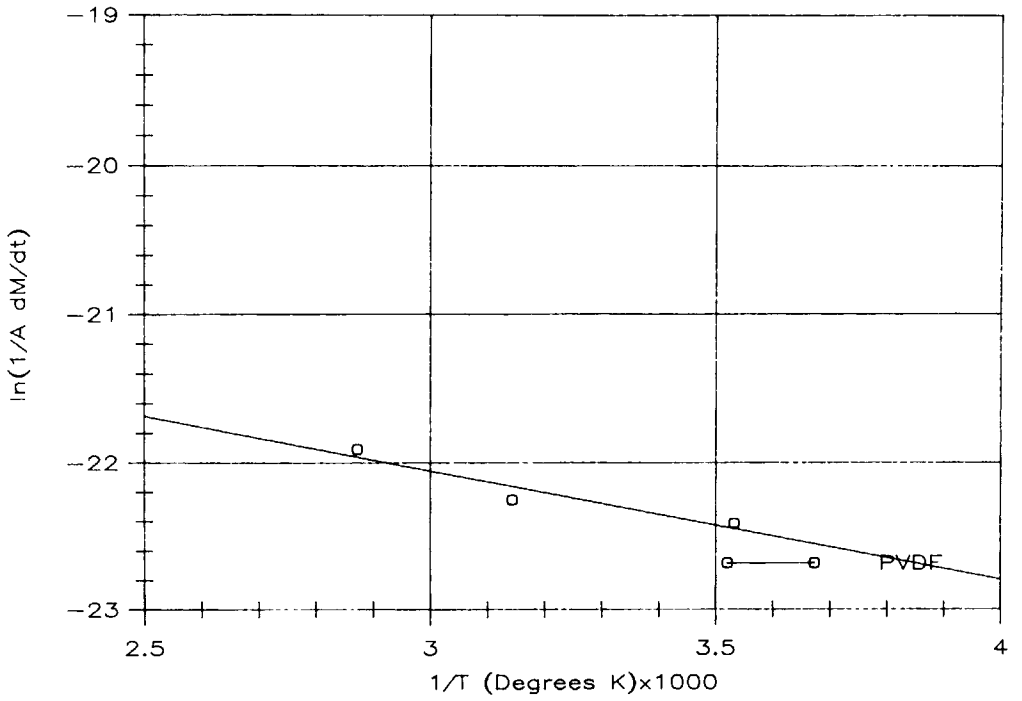


**Figure 5** Log (mass loss per area) vs. 1/T for PVDF.

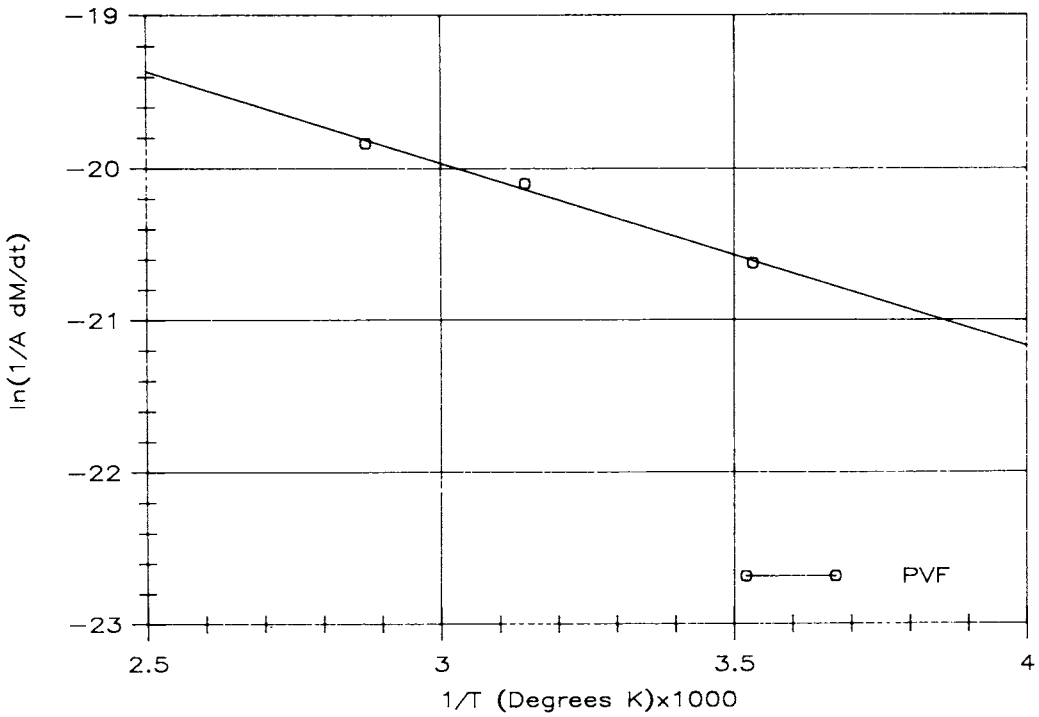


**Figure 6** Log (mass loss per area) vs. 1/T for PVF.

where $T > To : b = b_L$

$T < To : b = \text{bg},$

but $f = fce^{-E'/RT}$ (6)

where $fc$ is a constant, $T$ is the absolute temperature, and $E'$ is the free volume activation energy. This representation is made in order that an equivalent activation energy might be produced to describe the

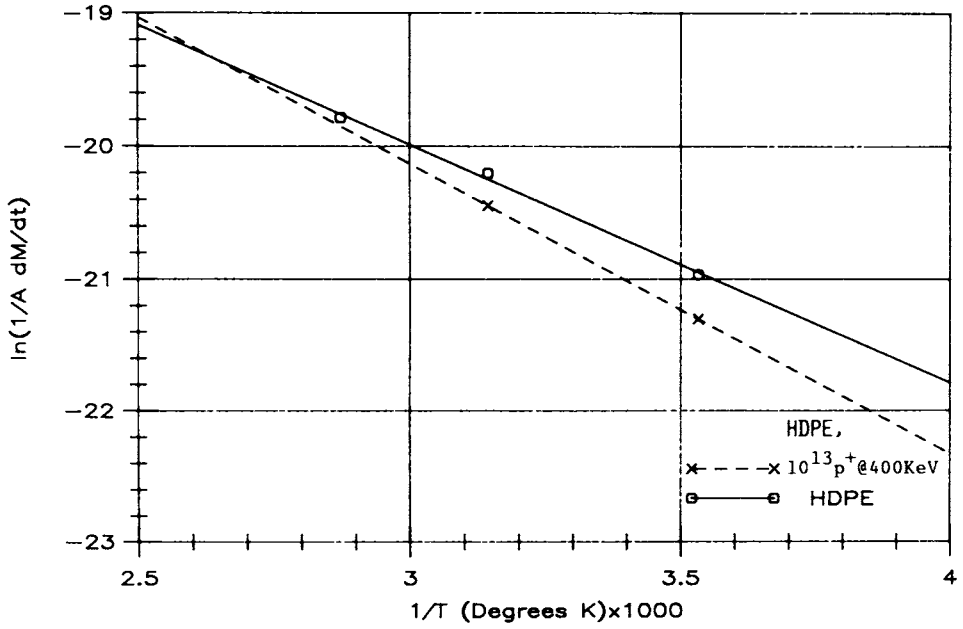


**Figure 7** Log (mass loss per area) vs. 1/T for HDPE, irradiated and unirradiated.

**Table II Activation Energy for Atomic Oxygen Exposed Polymers**

| Material | Activation Energy (KJ/mole) |
|---|---|
| Polytetrafluoroethylene | 1.0 |
| FEP | 3.0 |
| PVDF | 6.2 |
| Mylar | 9.8 ± 1.5 |
| PVF | 10.0 |
| Kapton | 14.0 |
| @ $10^{13}$ $p^+$, 400 KeV | 10.8 |
| Polyethylene | |
| UHMWPE | 13.3 |
| HDPE | 14.9 |
| @ 2 $19^{13}$ $p^+$, 400 KeV | 18.3 |
| LDPE | 14.1 |
| 119 K MWPE | 11.5 |
| 50 K MWPE | 12.0 |
| Polycarbonate | 15.4 |
| Nylon 6 | 19.1 |
| @ $10^{13}$ $p^+$, 400 KeV | 31.9 |
| Epoxy 956 | |
| @ 6 ± 1 h cure | 22.0 |
| @ 24 ± 2 h cure[a] | 17.4 |
| @ 48 ± 2 h cure | 22.1 |
| @ 72 ± 2 h cure | 23.6 |
| Epoxy 507 | |
| @ 6 ± 1 h cure | 17.9 |
| @ 24 ± 1 h cure | 19.6 |
| Polypropylene | 28.9 |
| PMMA | |
| 300 K | 21.1 |
| 1400 K | 48.8 |
| Polystyrene | |
| 760 K | 8.4 |
| 2610 K | 14.1 |
| Dimethyl silicone | Indeterminate |

[a] Considerable absorbed moisture in samples.

temperature rate effect within a limited temperature region.

Fractional free volume calculations were made from eq. (5), primarily using data from Aharoni[37,38] and Koo[39] and literature/measured values of $To$, which was chosen to be the glass transition temperature, $T_g$. By choosing $To = T_g$, we bias the analyses so that the $E'$ values are relative values. The value of $fo$, the fractional free volume at $T_g$, was taken to be 0.037, which was derived from packing density considerations of polymers modeled as a three-dimensional array of hard spheres.[40] These values were put into eq. (5) and free volume activation energies were generated for several polymers. A typical calculation was made for polyvinylidene fluoride, where the glass transition temperatures lay within the bulk material temperature range utilized here.

$$bg = fo/To = fo/T_g = 0.037/318°\text{K}$$
$$= 1.163 \times 10^{-4}\,°\text{K}^{-1}$$

Substituting $bg$ into equation (5)

$$f^{283°\text{K}} = 0.037 + 1.163 \times 10^{-4}(283\text{–}318) = 0.033$$

$b = (b_L - bg)$, where

$b$ = coefficient of free volume

expansion and $b_L = 2.83 \times 10^{-4}$

$$f^{348°\text{K}} = 0.037 + 2.83 \times 10^{-4}(348\text{–}318) = 0.455$$

The values of $f_{\circ T}$ are substituted into eq. (6) and the slope determined from the plot of $ln f$ vs. $1/T$. $E'$ was determined to be 4.05 KJ mole$^{-1}$ for PVDF.

A plot of these energies vs. the atomic oxygen activation energies is shown in Figure 8. $E'$ values were generated for the fluorinated materials, PE and Nylon. The equation for this relationship was $Ea = 2.02E'\text{–}3.37$. The mass loss rate (MLR) dependence upon $E'$ could be written according to:

$$\text{MLR} \alpha e^{-(-3.37/RT)} \times e^{-1.01\,E'/RT} \times e^{-1.01\,B'/RT},$$

which suggested that this process could involve a second order dependence on free volume (but left an unexplained temperature dependence). However, the correlation of $Ea$ with the diffusion activation energy was straightforward and offered one point of attack for attempting a detailed model of atomic oxygen attack on polymers.

The number of mass loss events per atomic oxygen atom, $\tau$, for materials at 45°C range from about three per ten thousand for the more stable fluorinated materials to about nine per thousand for the most reactive materials. The number of events, as expected, increased with increasing temperature. These numbers, for the estimated mass loss per event ($\delta m/\delta \epsilon$), accounted for only a small portion of the available atomic oxygen and implied that other processes occurred prior to, or in parallel with, these mass loss events. This would be the case even if $\delta m/\delta \epsilon$ had been underestimated by a factor of 10, which, in itself, would be unlikely. This suggested that removal of material by oxygen attack or by recombination of oxygen atoms was a more complex

**Table III Mass Loss vs Atomic Oxygen Flux for Selected Polymers**

| Polymer | Test Conditions | Mass Loss (mg @ ½ h) | AO Flux (#/m²/sec) |
|---|---|---|---|
| PVDF | 40 wt/800 mt/45°C | 0.206 ± 0.016 | $1.50 \times 10^{22}$ |
| PVDF | 60 wt/800 mt/45°C | 0.390 ± 0.020 | $3.13 \times 10^{22}$ |
| FEP | 40 wt/700–850 mt/45°C | 0.205 ± 0.008 | $< 1.50 \times 10^{22}$ |
| FEP | 60 wt/700–850 mt/45°C | 0.449 ± 0.048 | $< 3.13 \times 10^{22}$ |
| UHMWPE | 60 wt/600 mt/45°C | 2.301 ± 0.132 | $2.36 \times 10^{22}$ |
| UHMWPE | 60 wt/800 mt/45°C | 2.921 ± 0.252 | $3.13 \times 10^{22}$ |
| Nylon 6 | 40 wt/800 mt/45°C | 1.650 ± 0.008 | $1.50 \times 10^{22}$ |
| Nylon 6 | 40 wt/600 mt/45°C | 1.505 ± 0.072 | $< 1.50 \times 10^{22}$ |

**Table IV Mass Loss Equation Parameters**

| | $\phi$ | | | $\tau$ | | | $Ea$ |
|---|---|---|---|---|---|---|---|
| Material | 10°C | 45°C | 75°C | 10°C | 45°C | 75°C | (KJ/mole) |
| TFE | 0.00044 | 0.00042 | 0.00044 | 0.00028 | 0.00029 | 0.00031 | 1.0 |
| FEP | 0.0013 | 0.0013 | 0.0013 | 0.00035 | 0.00042 | 0.00045 | 3.0 |
| PVDF | 0.0053 | 0.0047 | 0.0054 | 0.00039 | 0.00046 | 0.00064 | 6.2 |
| Mylar | 0.202 | 0.202 | 0.202 | 0.0019 | 0.0032 | 0.0046 | 9.8 |
| PVF | 0.229 | 0.242 | 0.228 | 0.0032 | 0.0054 | 0.0071 | 10.0 |
| Polyethylene | | | | | | | |
| UHMWPE | 1.27 | 1.29 | 1.27 | 0.0045 | 0.0085 | 0.013 | 13.3 |
| HDPE | 2.18 | 2.32 | 2.16 | 0.0038 | 0.0081 | 0.012 | 14.9 |
| @ $10^{13}$ $p^+$ | 6.43 | 6.43 | — | 0.0027 | 0.0063 | — | 18.3 |
| LDPE | 1.64 | 1.63 | 1.65 | 0.0042 | 0.0080 | 0.013 | 14.1 |
| 119 K PE[a] | 0.457 | 0.344 | 0.457 | 0.0035 | 0.0045 | 0.0089 | 11.5 |
| 50 K PE | 0.718 | 0.778 | 0.710 | 0.0044 | 0.0083 | 0.011 | 12.0 |
| Lexan | 1.12 | 1.06 | 1.13 | 0.0017 | 0.0032 | 0.0057 | 15.4 |
| Nylon 6 | 10.88 | 11.34 | 10.82 | 0.0033 | 0.0084 | 0.0149 | 19.1 |
| @ $10^{13}$ $p^+$ | 907.7 | 929.3 | 907.4 | 0.0019 | 0.0054 | 0.0150 | 31.9 |
| Kapton | 0.24 | 0.24 | 0.24 | 0.0006 | 0.0012 | 0.0019 | 14.0 |
| @ $10^{13}$ $p^+$ | 0.08 | 0.08 | 0.07 | 0.0008 | 0.0014 | 0.0018 | 10.8 |
| Epoxy 956 | | | | | | | |
| @ 6 ± 1 h cure | 16.34 | 19.50 | 15.97 | 0.0014 | 0.0047 | 0.0079 | 22.0 |
| @ 24 ± 2 h[b] cure | 3.87 | 3.85 | 3.87 | 0.0025 | 0.0055 | 0.0097 | 17.4 |
| @ 48 ± 2 h cure | 14.34 | 12.64 | 14.56 | 0.0018 | 0.0042 | 0.0097 | 22.1 |
| @ 72 ± 2 h cure | 34.71 | 38.07 | 34.30 | 0.0016 | 0.0051 | 0.0097 | 23.6 |
| Epoxy 507 | | | | | | | |
| @ 6 ± 1 h cure | 4.67 | 5.04 | 4.57 | 0.0023 | 0.0058 | 0.0078 | 17.9 |
| @ 24 ± 1 h cure | 9.18 | 9.81 | 9.09 | 0.0022 | 0.0060 | 0.0100 | 19.6 |
| Polypropylene | 414 | 414 | — | 0.0019 | 0.0074 | — | 28.9 |
| Polystyrene | | | | | | | |
| 760 K | 0.050 | 0.047 | 0.051 | 0.0014 | 0.0020 | 0.0025 | 8.4 |
| 2610 K | 0.606 | 0.657 | 0.610 | 0.0015 | 0.0028 | 0.0047 | 14.1 |
| PMMA | | | | | | | |
| 300 K | 148 | 148[c] | — | 0.0193 | 0.0303[c] | — | 21.1 |
| 1400 K | 177 | 177$x$ | — | 0.0050[c] | 0.0174 | — | 48.8 |
| | $10^{4}$ [c] | $10^{4}$ | | | | | |

[a] Nonuniform surface areas.
[b] Sample contained considerable absorbed moisture.
[c] Data at 25°C.

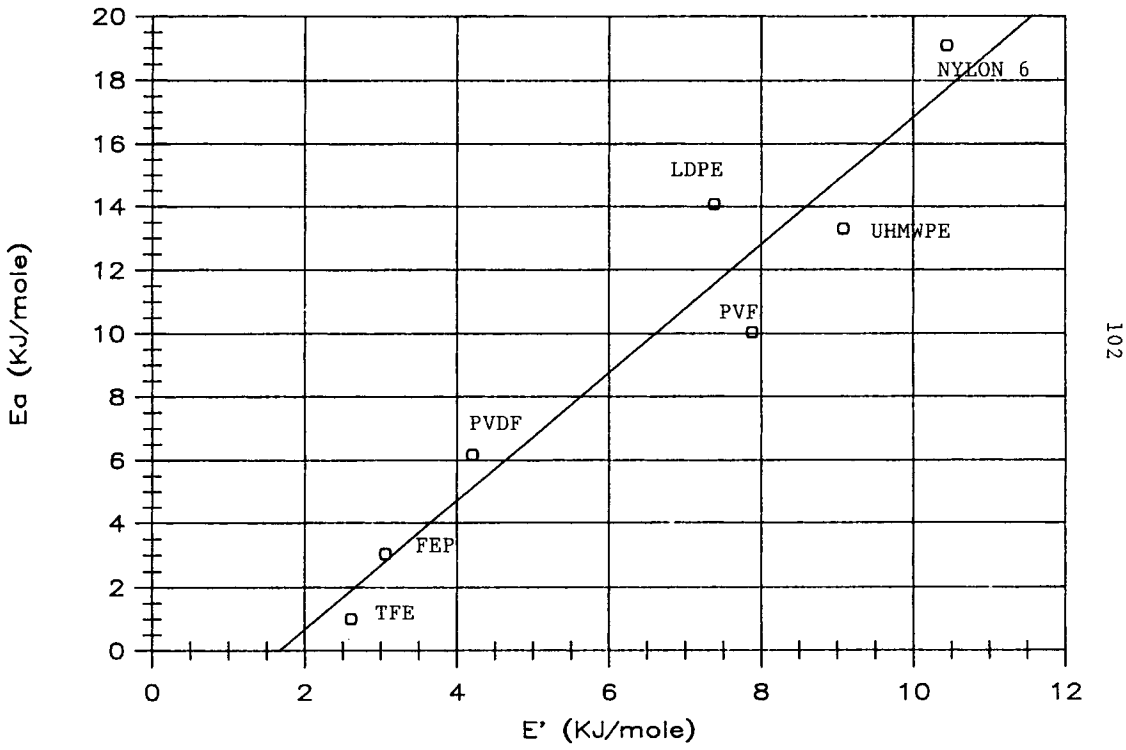


**Figure 8** Atomic oxygen activation energy vs. free volume activation energy.

process. There was essentially no change in mass loss events with type of polyethylene or with epoxy cure time, but small differences were noted in *Ea* and $\phi$. A decreasing trend in mass loss events occurred with Nylon 6 and high density polyethylene, which had been irradiated with 400 KeV protons to a fluence of $10^9/m^2$. Particle irradiation can cause crosslinking and/or chain scission to occur in poly-

**Table V Comparison of Activation Energy[a] for Diffusion of $O_2$, $N_2$, $H_2$, and He in Polymers with Atomic Oxygen Activation Energy**

| | Activation Energy for Diffusion, (KJ/mole) | | | | Activation Energy for Atomic Oxygen Attack |
|---|---|---|---|---|---|
| Polymer | $N_2$ | $O_2$ | $H_2$ | He | |
| TFE | 29.8 | 26.3 | — | — | 1.0 |
| FEP | 38.5 | 34.7 | 25.1 | 20.9 | 3.0 |
| | 29.3 | 25.1 | | | |
| PS | — | 37.7 | 16.7 | 13.0 | 8.4 |
| | | | | | 14.1 |
| Mylar | 58.7 | 50.6 | — | 20.1 | 9.5 |
| Kapton | 31.0 | — | — | — | 13.1 |
| LDPE | 50.3 | 40.2 | 33.5 | 24.7 | 14.1 |
| HDPE | 39.8 | 36.8 | — | 23.4 | 15.0 |
| PC | — | 32.2 | 20.9 | — | 15.4 |
| Nylon 6 | 46.1 | 33.5 | 31.5 | — | 19.1 |
| PP | 41.9 | 36.5 | 34.7 | 30.6 | 28.9 |
| PMMA | 20.9 | — | — | — | 21.0 |
| | 31.8 | | | | 48.0 |

[a] Data from references 46, 47, 48.

mers.[41] More specifically, irradiation, which results in crosslinking, tended to restrict molecular mobility. This made diffusion more difficult, and thereafter the rate of reaction was reduced.

The range of $\phi$, the frequency factor, for these materials extended over seven orders of magnitude with the most stable materials having the lowest values. Magnitude of these data appeared to have been characteristic for a type of polymer and probably represented a fundamental polymer response.

The examination of mass loss rates has indicated that the stability of the polymer increased with increased backbone bond strength and that pendent structures can protect the backbone. Further, if it is assumed that these rate processes are increased with pendent structure vibrational frequency, then the following approach could be correlated with $p$, provided that it did not far exceed 1 in value. The rationale underlying this calculation was the physical blocking of AO to the polymer backbone. Using the covalent radii for hydrogen, carbon, and fluorine, from Sanderson, of 0.32 Å, 0.77 Å, and 1.61 Å, respectively, and the vibrational energies of 35.4 KJ/mole for C—H and 15.6 KJ/mole for C—F, as the C—C backbone attached bonds,[42] $p$ can be constructed to be:

$$\phi = ae^{-X}$$

where $X = Eb/Ev \times R/2L \times \Omega$

where $Eb$ is equal to the C—C bond energy of 347 KJ/mole, $Ev$ the vibrational energy taken from IR data, $R$ the radius of the attached atom, $L$ the bond length to the polymer backbone, and $\Omega$, an order factor defined as $O \leq \Omega \leq 1$. Assuming $\Omega = 1$ and $a \approx 1$,

For TFE:

$$X = (347/15.6) \times (1.61/2.43) \times 1/2 = 7.4$$

$$\phi = e^{-X} = 0.0006$$

For PE:

$$X = (347/35.4) \times (.32/1.09) \times 1/2 = 1.43$$

$$\phi = .24$$

Generated values of $\phi$ for polyethylene and TFE agreed with experimentally determined $\phi$ from Table IV. However, values were found to exceed 1 for several polymers, so this analysis was not considered adequate for correlation to $\phi$.

A plot of activation energy versus $ln\phi$ in Figure 9 indicated that they were related and, as suggested by Stannett,[43] may be approximately the same function in the appropriate variables. The preexponential factor for diffusion has been formulated by Eyring to be a function of the average diffusional jump length, $\tau$, and the entropy of activation $\triangle S$.

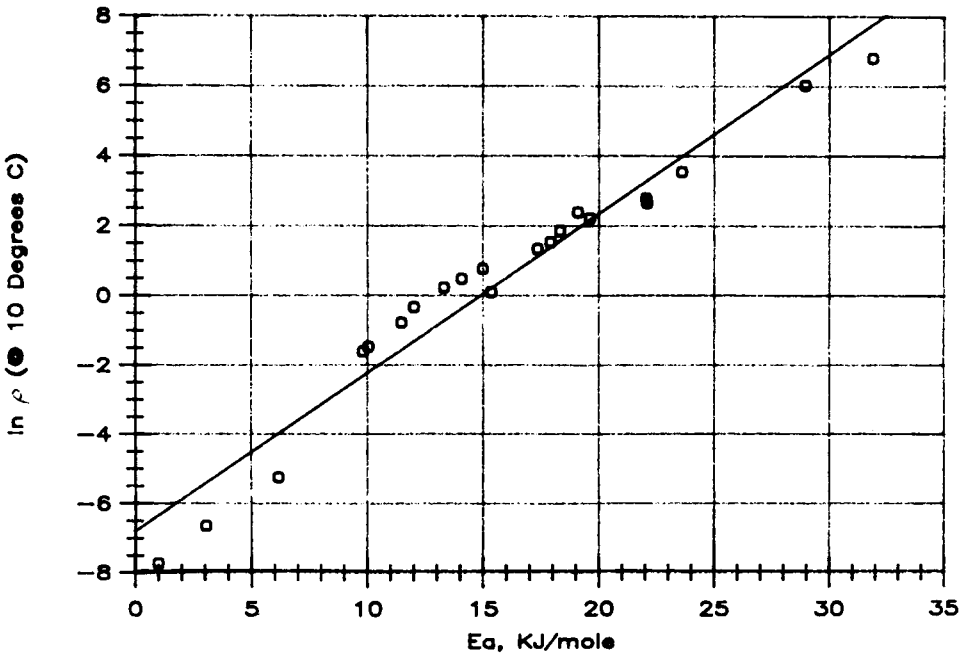


**Figure 9** Natural logarithm of frequency factor vs. atomic oxygen activation energy.

**Table VI Material Effects on Mass Loss Equation Parameters**

| Effect | Materials | Mass Loss Equation Parameters $\phi$ | $\tau$ | $Ea$ |
|---|---|---|---|---|
| Crosslinking | Epoxies | Increase with cure | Constant | Increase with cure |
| | Nylon 6 HDPE | Increase with irradiation | Decrease with irradiation | Increase with irradiation |
| Chain scission | Kapton | Decrease with irradiation | Increase with irradiation | Decrease with irradiation |
| Mol wt | PE, PS, PMMA | Increase with mol wt | Constant to mixed | Increase with mol wt |
| Fluorination | TFE, FEP, PVDF, PVF | Decrease with increasing $F$ | Decrease with increased $F$ | Decrease with increased $F$ |
| Branching | PE, PP, PS, PMMA | Relative to PE-decrease with ring structure, increase with methyl, long side groups | Relative to PE-decrease with methyl, ring structure, increase with long side groups | Relative to PE-decrease with ring structure, increase with methyl, long side groups |

The polyethylene, epoxy, polystyrene, and PMMA data of Table V show a tendency of $\phi$ to increase with $Ea$ under conditions that favor a decrease in free volume. These conditions included increased crosslinking and increased mol wt. The results these effects on the activation entropy is unclear, but these effects would be expected to increase the jump length. Tables VI and VII contain summaries of the effects of crosslinking, mol wt, branching, fluorination, and bond strengths reflected in the mass loss equation parameters.

The primary bonding magnitude was an important factor in the resistance of a material to atomic oxygen attack. Ionic bonded materials and strong covalent bonded nonpolymers show little or no reactivity. Metals showed a mixed reactivity with silver and osmium being highly reactive. Most other metals, while being reactive, tended to be self-passivating. While the covalent bonded polymers were reactive with C—C backbone bond strengths of 347 KJ/mole, some variation existed in the covalent backbone bond strength magnitudes, with Kapton having a C—N bond strength of 293 KJ/mole and dimethyl silicone having a Si—O bond strength of 494 KJ/mole. Other factors affected the overall reactivity of these materials, such as the formation of $SiO_2$, which shielded the silicone polymer and the inclusion of a ring structure, which added stability to the backbone of Kapton. Nylon 6 contained intermolecular hydrogen bonds, which was probably responsible for the activation energy of atomic oxygen diffusion being somewhat higher than that for polyethylene. However, this material contained the relatively weak C—N bond, thus making it more

**Table VII Bonding Effects on Mass Loss Equation Parameters**

| Bond | Materials | Mass Loss Equation Parameters $\phi$ | $\tau$ | $Ea$ |
|---|---|---|---|---|
| Primary | $MgF_2$ | | Indeterminate | |
| | NaCl | | Indeterminate | |
| | Silver | — | — | 9.8–27.0 |
| | Other metals | | Mixed reactivity | |
| | PE | 1–2 | 0.0080 | 11–15 |
| | Dimethyl silicone | | Indeterminate | |
| Hydrogen | Nylon 6 | 11 | 0.0054 | 19.1 |
| Van der Waals | PE | 1–2 | 0.0080 | 11–15 |
| | TFE | 0.00044 | 0.00029 | 1.0 |
| | PVDF | 0.0050 | 0.00046 | 6.2 |

reactive. While Van der Waals bonding applied to all of the polymers, it represented a weak bond on the order of less than about 8 KJ/mole. In the symmetrical polymers, which were easier to analyze, the approach distance of atoms determined the magnitude of these forces and, as can be seen from the data of Table VII, those forces, as reflected in the activation energies of apparent diffusion, were less for the fully fluorinated materials. (The fluorine atom is greater in diameter than the hydrogen atom.) The mix of H and F atoms, attached to a polymer backbone, yielded an activation energy between that of PE and TFE.

Using the mass loss rate, eq. (4), the mass losses measured for the STS-8 flight samples of Kapton and polyethylene were calculated. The on-orbit values for both these materials were essentially the same, but their temperatures were unknown. Attempts were made to control on-orbit materials at 23, 70, and 120°C, but thermal labels indicated that these temperatures were exceeded. Calculated mass loss values were within a factor of 2 of the measured values. Another element affecting accuracy of calculations was that the on-orbit flux was known only within an order of magnitude.

## Effect of Annealing/Quenching on the Mass Loss Rate of Lexan

The effect of structure order on the mass loss rate was studied using polycarbonate (Lexan). This material was annealed at and above the glass transition temperature for .5 h. It then underwent rapid quenching in ice water, air quenching, or was slowly cooled to ambient temperature. Following the quench process, it was exposed to atomic oxygen while being held at 10 or 15°C. Mass loss for the specific material conditions and plasma exposure are described in Table VIII. The data show a small trend of decreased mass loss for all the annealed and quenched samples. Statistically, no distinction was seen in the mass loss rates within the various annealed/quenched conditions. Some ordering of polycarbonate molecules is known to have occurred near the glass transition temperature. Further, the maximum rate of crystallization occurred near 190°C with spherulitic structures formed at this temperature over several days.[44] The reduced mass loss rate observed here could be accounted for through a more ordered structure that would be more dense, less permeable, brought about by the annealing/quenching process.

**Table VIII Effect of Annealing/Quenching on the Mass Loss Response of Lexan in Atomic Oxygen**

| Mass Loss (mg) at T°C/800 mT/60 Watts | Sample Treatment Prior to Plasma Exposure |
|---|---|
| 10°C: 0.711 ± 0.026 | Control |
| 10°C: 0.617 ± 0.033 | Heated to 149°C, quenched to 0°C, vacuum dried |
| 10°C: 0.645[a] | Heated to 198°C, air quenched to 23°C |
| 15°C: 0.758[a] | Control |
| 15°C: 0.661 ± 0.75 | Heated to 210°C, quenched to 0°C, vacuum dried |
| 15°C: 0.688[a] | Heated to 210°C, slowly cooled to ambient temperature |

[a] One sample tested.

**Table IX ESCA Data for Polymer Materials**

| Material | $N_c/N_o$ | $N_c/N_f$ | $N_c/N_n$ |
|---|---|---|---|
| Polyethylene | | | |
| (C) | 29.3 | — | — |
| (Exp) | 9.89 | | |
| Polyvinyl fluoride | | | |
| (C) | 36.2 | 3.18 | — |
| (Exp) | 11.7 | 4.56 | — |
| Fluorinated ethylene propylene copolymer | | | |
| (C) | — | 0.596 | 6.75 |
| (Exp) | 19.1 | 0.687 | — |
| Polytetrafluorethylene | | | |
| (C) | | 0.610 | 3.13 |
| (Exp) | 12.7 | 0.875 | 4.55 |

## Surface Analysis by ESCA

Surface analyses by electron spectroscopy for chemical analyses (ESCA) were used to characterize selected material samples. In this evaluation, the material was irradiated with monoenergetic x-rays and the resulting photoelectrons were energy analyzed to determine their binding energies to the surface atoms. The analysis emphasized here was the determination of the ratios of surface constituent elements, which provided an indication of the bonds more readily attacked and of the material lost from the sample surface. Five polymeric materials were examined by ESCA by the Chemical Engineering Department at Auburn and the results of that analysis are provided in Table IX. Survey scans were

used to determine the elemental composition of the surface. Major peaks were then evaluated individually to obtain a quantitative evaluation of the surface composition.

All data showed oxygen to be increased in the polymer surface as a result of plasma exposure. The more fully fluorinated, exposed materials, FEP and TFE, contained more unreacted oxygen atoms per fluorine atom. This could, perhaps, be partially explained by the relative electrophilic nature of oxygen and fluorine. While oxygen can readily diffuse into the surface of these materials, for reaction and mass loss to occur, the oxygen and fluorine, which are both highly electronegative, must compete for the same bonds. The ratios of carbon to fluorine indicated a small increase with exposure. As —CH/CF— and $-CF_2-$ groups were lost, the carbon to fluorine ratio slightly increased, which accounted for the exposure ratios. From the standpoint of material attack, since the fluorine tended to shield the carbon–carbon backbone, in the more fluorinated materials the fluorine must essentially be removed to remove a carbon atom, thus suggesting that this ratio would not be expected to vary much from the unexposed sample. The presence of nitrogen on the FEP and TFE materials was considered to be the result of surface contamination. Chemical analyses indicated that the nitrogen content for the total sample was far less than surface analysis indications.[45]

Three additional materials, HDPE, PVDF, and Kapton, were examined via ESCA by Dr. Brent Carter of the Georgia Tech Materials Engineering faculty. These materials included controls and oxygen plasma exposures for 30 min and 95 min. All samples showed a considerable increase in the amount of O1s oxygen upon exposure. Kapton indicated an increase in C=O/C—O=O on both samples, which were exposed for different durations. No distinctions were found in the exposed samples as a result of the length of exposure. A slight concentration change from 54 and 46% for $CH_2$ and $CF_2$, respectively, to 51 and 49% was noted from the control to the 95 min exposed sample, but this was not considered to be significant. A shift in the O1s and C1s peaks in the exposed samples indicated the formation of O—C=O or C=O. These findings are consistent with the work of Clark and Dilks,[2] Egitto et al.,[46] and Turban and Rapeaux.[47] Further, these findings are consistent with those of Liang et al.,[48] upon examination of polyethylene flown on STS-8.

**Table X Nominal Mass Spectrometer Data for TFE and PVF**

| Material | Atomic Mass Unit | Partial Pressure (%) |
|---|---|---|
| TFE | 31 (CF)[a] | 0.57 |
| | 48 (CHFO) | 0.05 |
| | 20 (HF) | 0.04 |
| | 47 (CFO) | 0.02 |
| PVF | 20 (HF) | 11.4 |
| | 48 (CHFO) | 0.01 |

[a] AMU 31 interpreted as CF, which may not be thermodynamically possible for duration to be seen in mass spectrometer.

## Residual Gas Analyses

Mass spectra data was collected on five polymers during oxygen plasma exposure. This data was collected during a 30 min exposure period of each polymer. The major gas species, as expected, was molecular oxygen, water vapor, carbon monoxide, and carbon dioxide, determined for exposure of the hydrocarbon polymers. Species present, other than molecular oxygen, in the background spectra were expected. No atomic oxygen was detected, as expected, since it was such a reactive species. The chamber was considered "dirty" relative to high vacuum chambers used for contamination studies. Periodically, the chamber was opened to ambient air during weighing of samples and water vapor collected on the chamber surfaces. Materials, such as Kapton, Mylar and Polyethylene, were primarily carbon and hydrogen structures, so that their dissolution into AMU of less than about 50 could not be discriminated from the background species. Essentially, no AMU were found above 55. If any large molecular species left the polymer surface, they may have undergone reactions in the gas phase and the mass spectrometer would not have detected it. Although background mass spectra with no sample were run in the chamber, this could not be subtracted from spectra with sample to give definitive data, based on the above aspects and the fact that the sampling pressures could not be precisely controlled. Consequently, no attempt was made to analyze extensively the gases by accounting for background gases. The RGA data for TFE and PVF are included in Table X. The fluorine atom was not found in the background spectra so that the presence of fragments containing fluorine could easily be discriminated. Carbon/fluorine/oxygen fragments were found at various AMU less than 50 and in small quantities.

The values of $\delta m/\delta \epsilon$ were assumed to lie between 14 and 50 AMU, with TFE and FEP assigned at 50 AMU based on ($-CF_2-$), PVDF assigned at 31 AMU (average of $-CH_2-$ and $-CF_2-$), and the remaining hydrocarbons given values from 14 to 18 AMU. These values were estimated from gas reaction studies of molecules, as mentioned previously. The RGA data obtained here supported this assumption.

## FTIR Analyses

Fourier Transform infrared analysis was performed on polyethylene samples using a Mattson Cygnus 100 Fourier Transform Infrared Spectrometer. These analyses were performed via contract to the author. The initial evaluations failed to show any differences between the control and atomic oxygen exposed samples. At that point, an attenuated total reflectance attachment (ATR) was used to acquire the surface spectra. In this analysis, the depth of penetration depended upon the angle of incidence, the wavelength of light, and on the relative refractive index of the sample and the ATR crystal. In this analysis, the KRS-5 crystal was used. This crystal has a high refractive index in order to minimize the critical angle ($\sin^{-1} n_2/n_1$, where $n_1$ is the refractive index of the ATR crystal and $n_2$ is the refractive index of the sample). As the angle of incidence decreased, the depth of penetration increased as long as the angle exceeded the critical angle.

The FTIR spectra were shown in the region from 2000 to 500 $cm^{-1}$, since the ATR beam depth penetration decreased with increasing wavenumber and, therefore, the spectrum was less intense and noisier in the 2700 to 3000 $cm^{-1}$ region. At an angle of incidence of 35 degrees, an intense band appeared at 842 $cm^{-1}$ on the exposed sides of the polyethylene samples. It also appeared at a considerably reduced

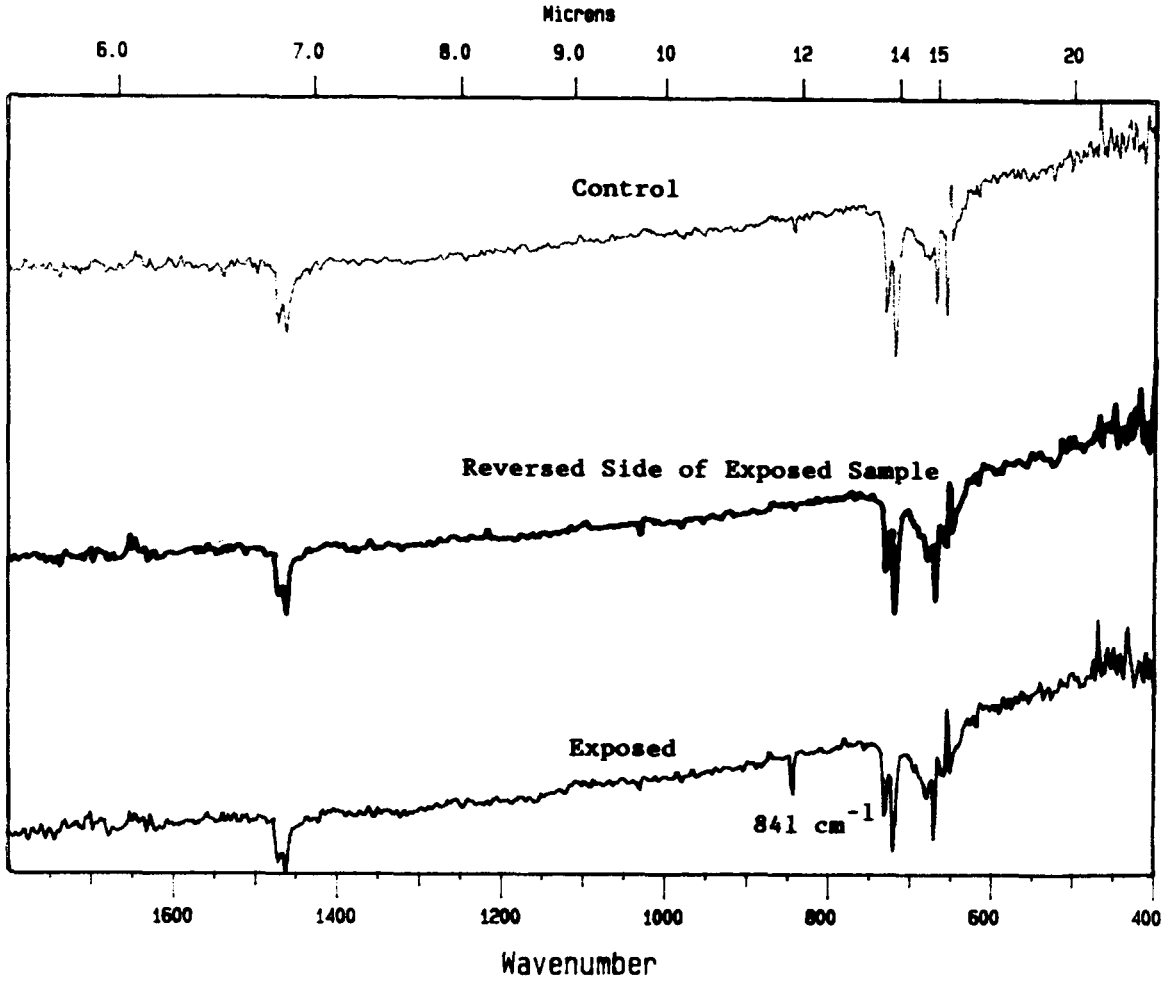


**Figure 10** FTIR spectra of HDPE.

intensity of the HDPE control sample and on the unexposed side of the LDPE sample. It is suspected that the reaction responsible for this peak may occur in air also, but to a lesser extent. This band corresponded to a C=C band. It was surmised that the band could have arisen as a result of the following reaction paths. The atomic oxygen could have literally stripped a carbon out of the polyethylene chain and the chain reform with a double bond in this position. CO would then be given off. Another possible explanation for the reaction would be for the oxygen to have formed a C—O bond as an inter-

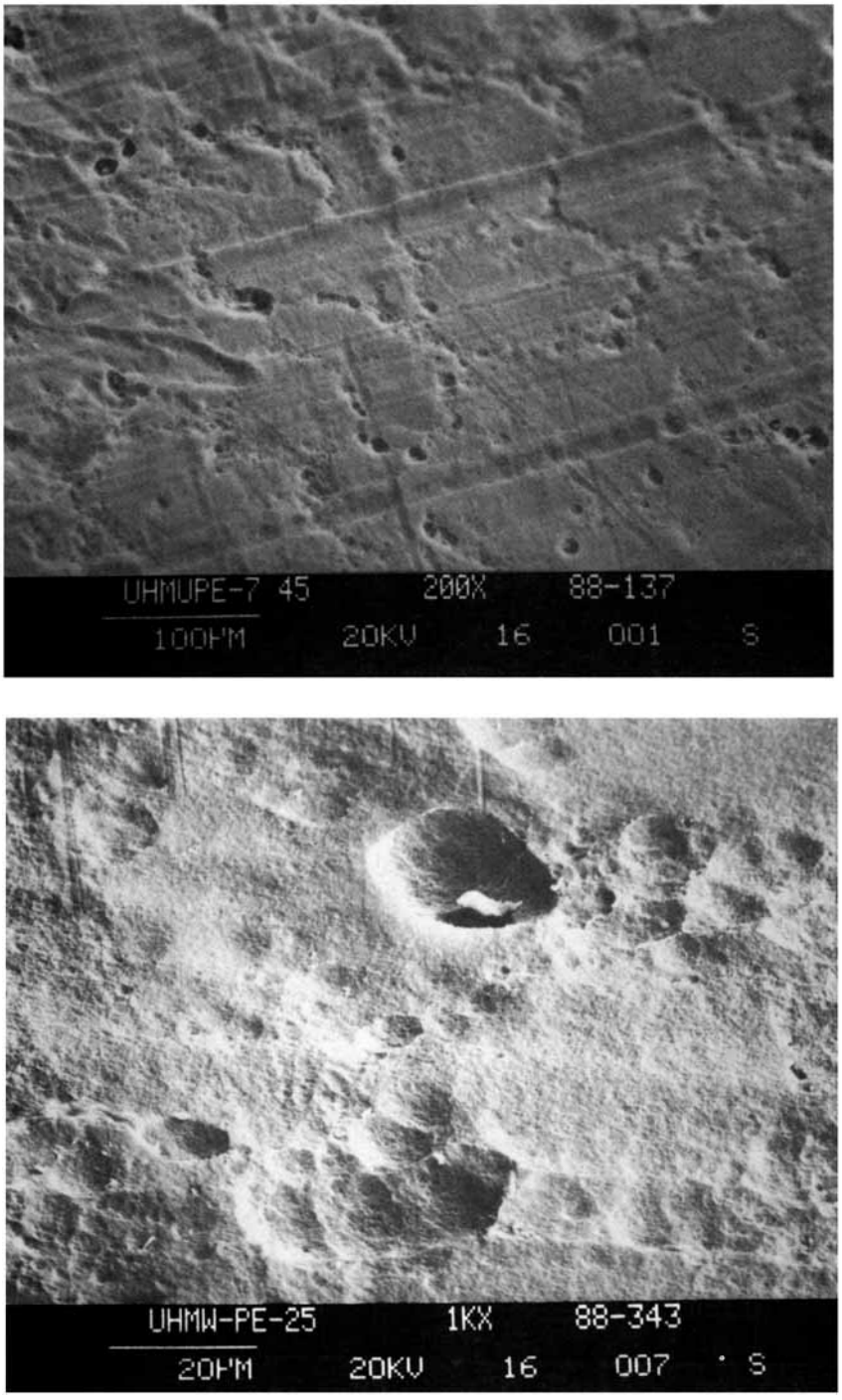


**Figure 11** Atomic oxygen exposed UHMWPE.

mediate, and then to have had it react with another oxygen to form $O_2$. The extra electrons would then have formed a double bond at that position. The FTIR spectra for HDPE for the exposed side, the reverse side, and the control sample are shown in Figure 10.

## Gel Permeation Chromatography Analyses

Attempts were made to measure the various mol wts of plasma exposed polyethylene. The only information that could be inferred from the GPC work is that there were no polymer fragments created that

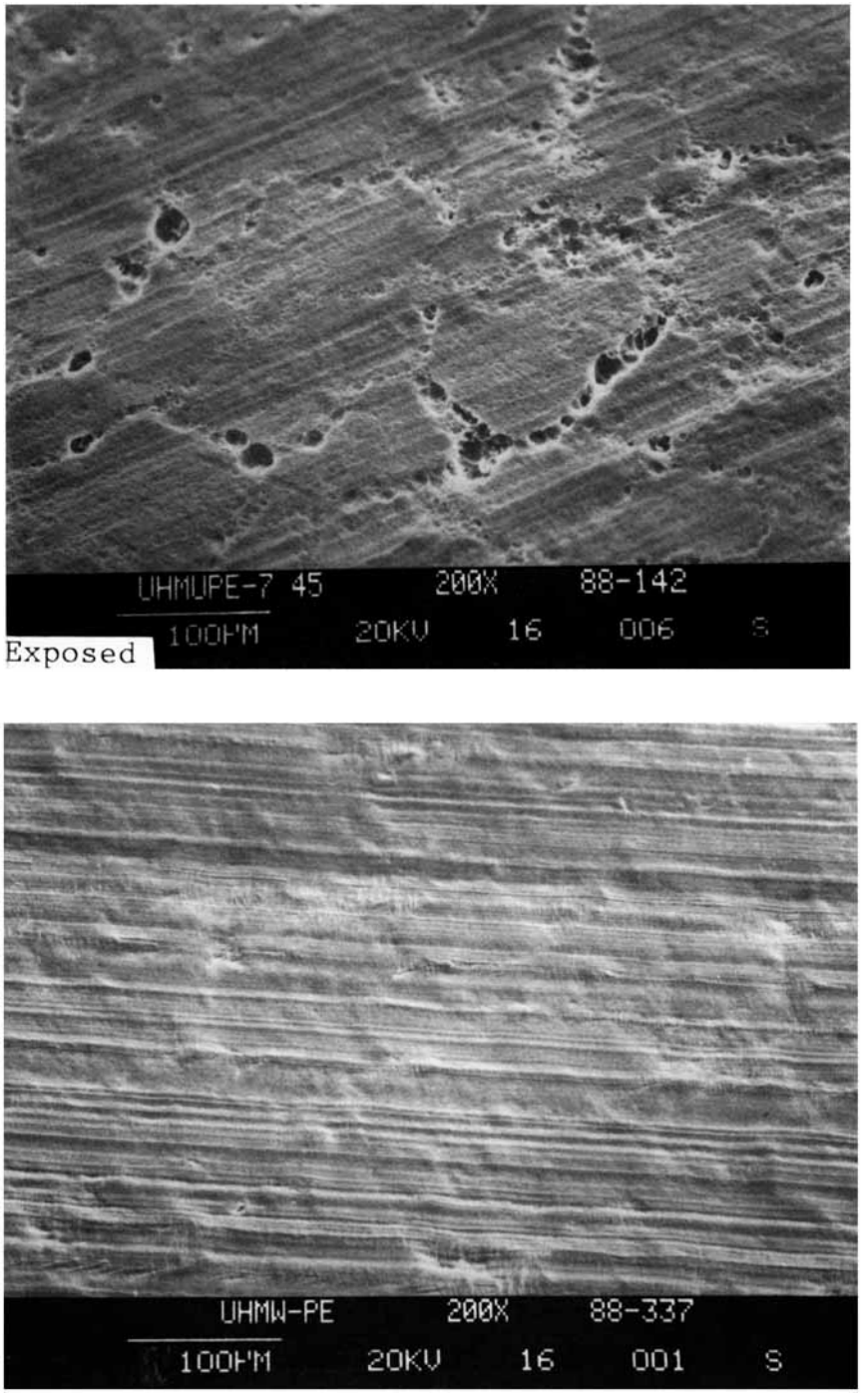


**Figure 12** Atomic oxygen exposed and control UHMWPE samples.

would be small enough in chain length and mol wt to have been solubilized at ambient temperature. This was consistent with the observations that the plasma exposure caused weight loss and that the FTIR analysis only supports the reformation of chain backbone after plasma exposure with no evidence of oxygen incorporation.

## Surface Characteristics

The surface features of oxygen plasma exposed materials were studied from scanning electron microscopy (SEM) photographs. Selected SEM photographs of oxygen plasma exposed surfaces and flight experiment samples are shown in Figures 11–18.

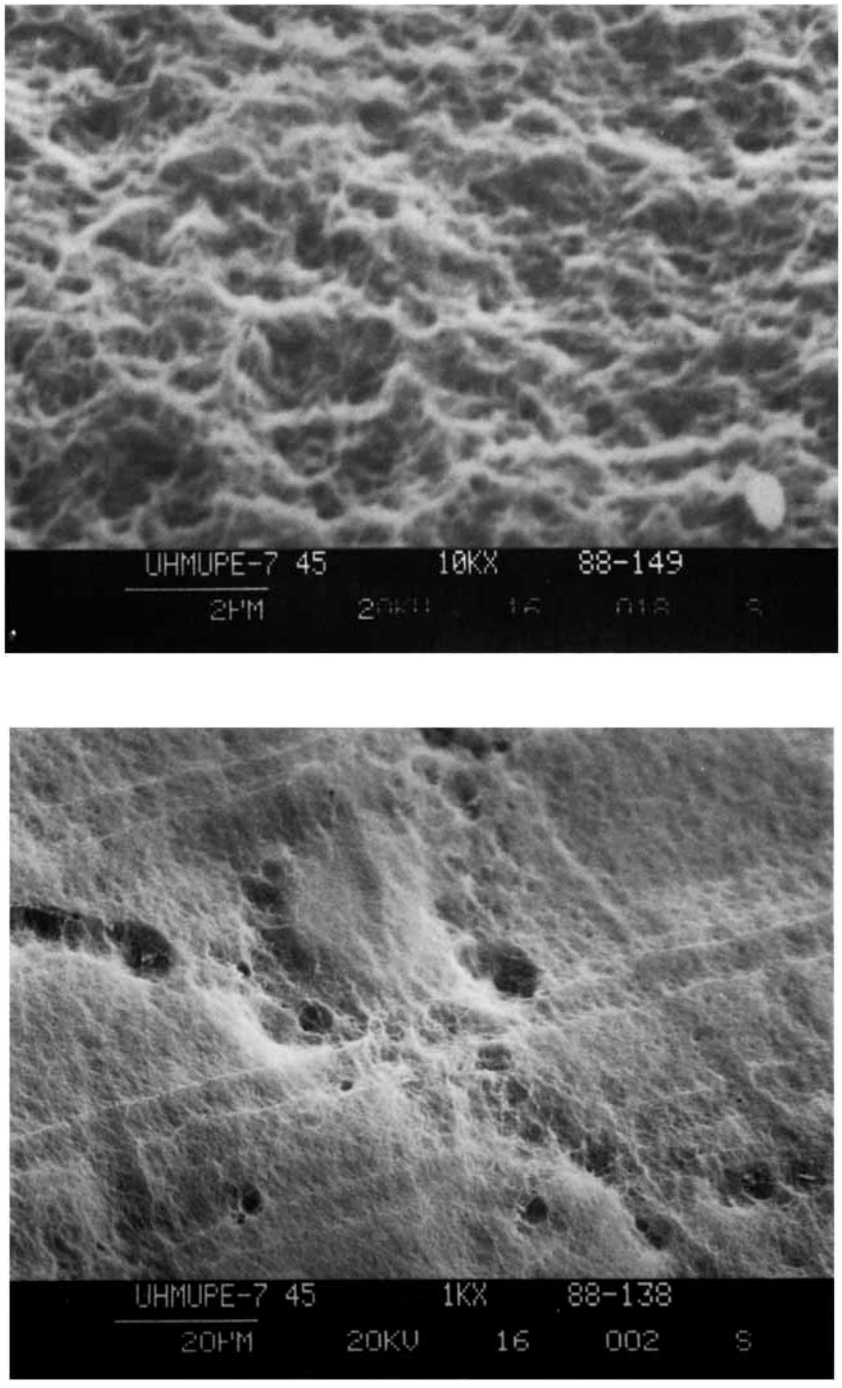


**Figure 13** Atomic oxygen exposed UHMWPE.

The polymer surfaces, exposed to the Plasmod produced thermal atomic oxygen at pressures of 800 to 1000 millitorr, generally showed surface features of cones, etches, and fiberous patterns similar to that seen in ion etched polymers. A comparison of flight to Plasmod exposed surfaces showed surface modulation to be more pronounced in the flight materials.

All of the commercially obtained polyethylene films have shown pits on or near the surface in the as-received materials (Figs. 11 and 12). In the UHMWPE, these pits, which appear in patterns, lie

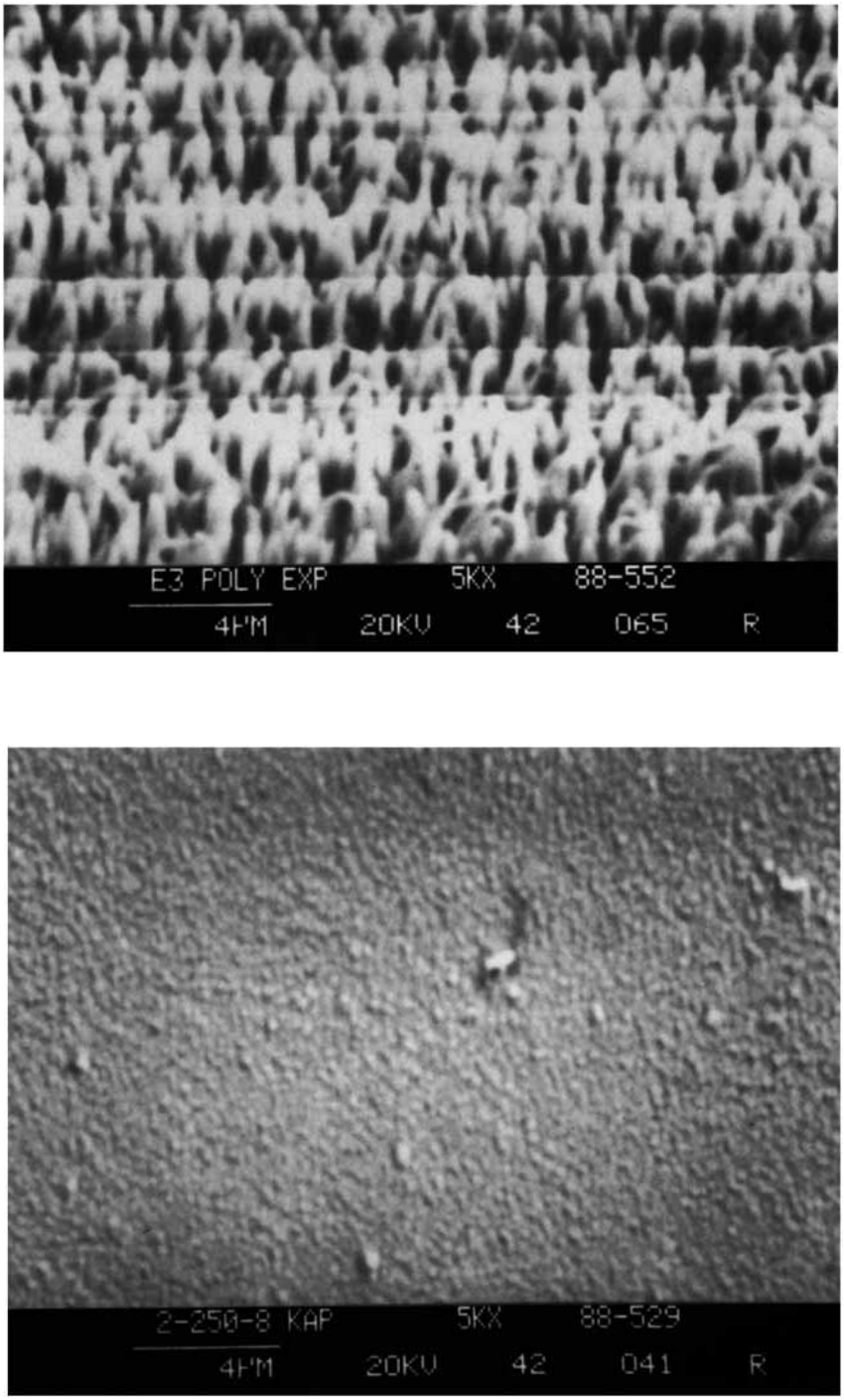


**Figure 14** Flight exposed PE (top) and Kapton (bottom).

just under the surface, as noted in the SEM of the unexposed material. No identification with respect to structure could be made for the pit pattern. The porous textured features, evident in the nonpitted areas, and shown in Figure 13, are characteristic of all the polyethylene samples exposed in the Plasmod system. In contrast to these features, STS-8 flight samples of PE (Fig. 14), with specific directional orientation to the atomic oxygen, showed closely spaced cone features with aspects ratios of about 10.

Surface features of Plasmod exposed Kapton were barely discernible, even at 100 K magnification (Fig.

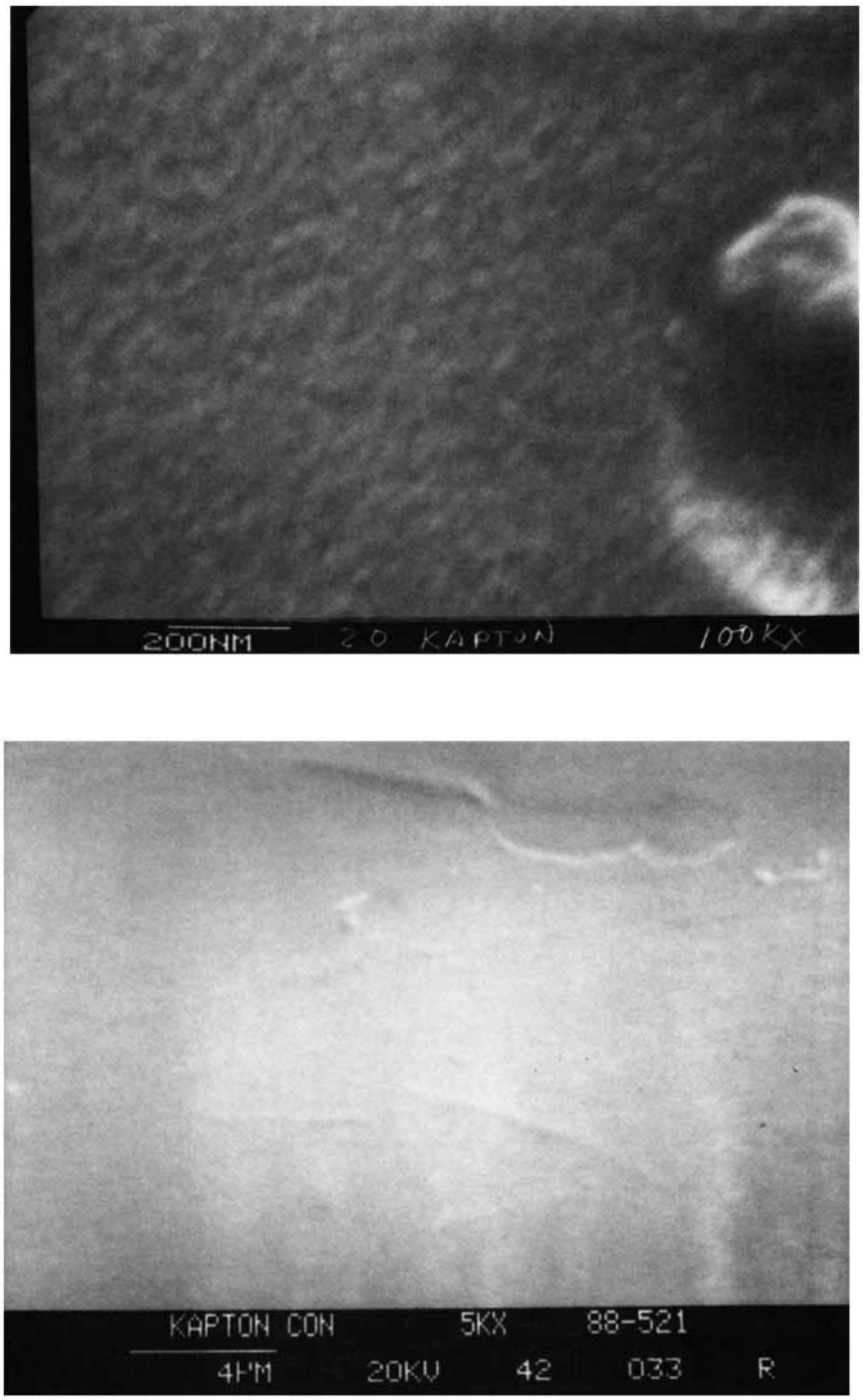


**Figure 15** Atomic oxygen exposed (top) and control (bottom) Kapton.

15). However, the structure seemed to be similar to that obtained on STS-5 flight exposed Kapton (Fig. 14), where the 5 eV atomic oxygen was allowed to impinge on the surfaces of various angles over 180 degrees. Mylar, exposed on STS-5 where atomic oxygen was omnidirectional, showed evidence of residual material on the surface. The Plasmod exposed Mylar gave a similar appearance. The surface residue could not be identified. However, it was noted that control Mylar (Fig. 16) contains similar concentrations of material. Plasmod exposed polyvinyl fluoride surfaces showed separated small cones, and ex-

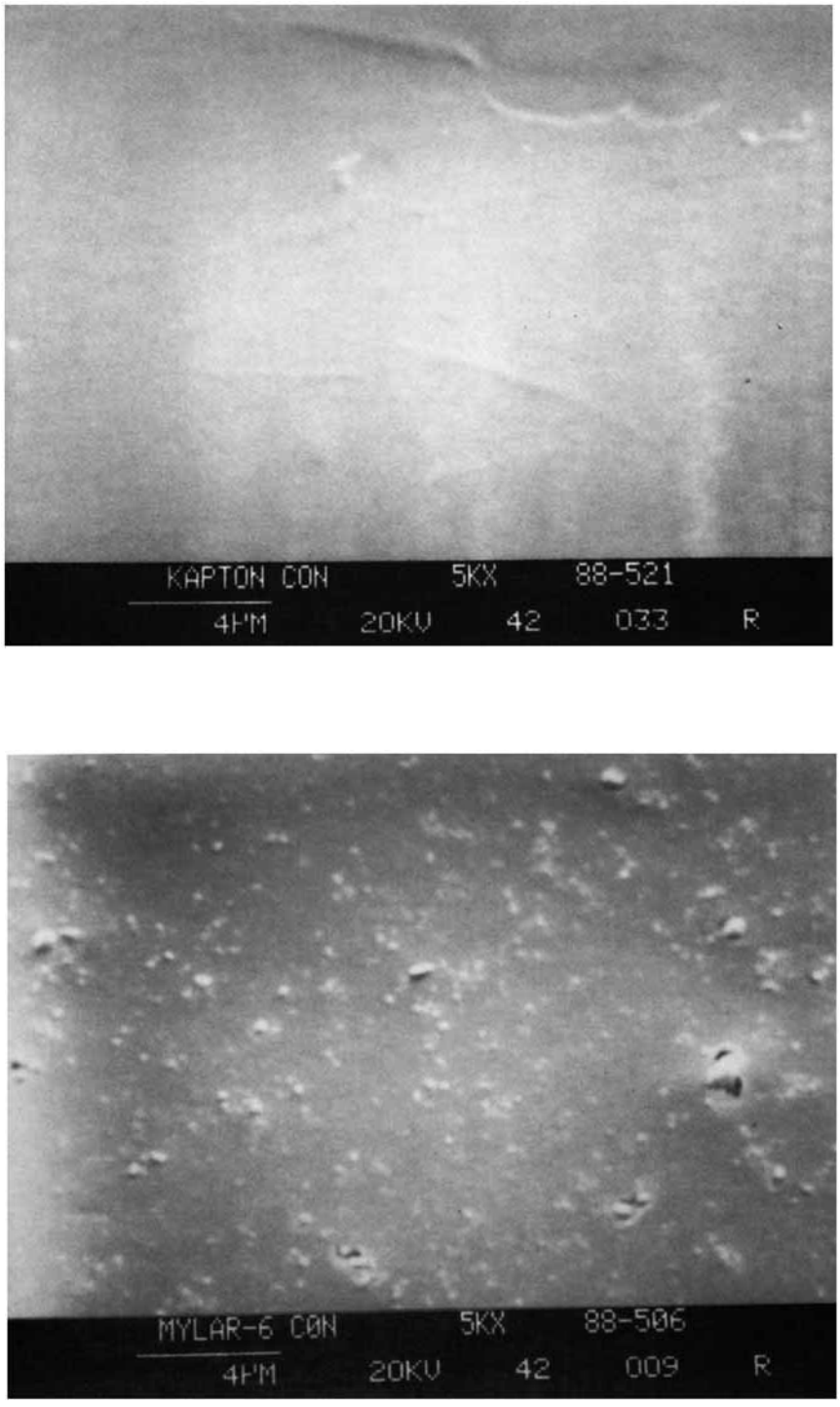


**Figure 16** Flight exposed (top) and control (bottom) Mylar.

posed polytetrafluorethylene showed the development of pores with the remaining material having a fine fibrous structure. No flight exposed materials were available for PVF, and flight surfaces of TFE from the Solar Maximum Mission satellite[46] have shown spaced cones with aspect ratios of 1 or less.

The surface morphologies observed for these materials showed a variety of structures, which were peculiar to the individual materials. Structures in the flight exposed materials were more pronounced, and differed in features. The flight materials were exposed under different environmental conditions:

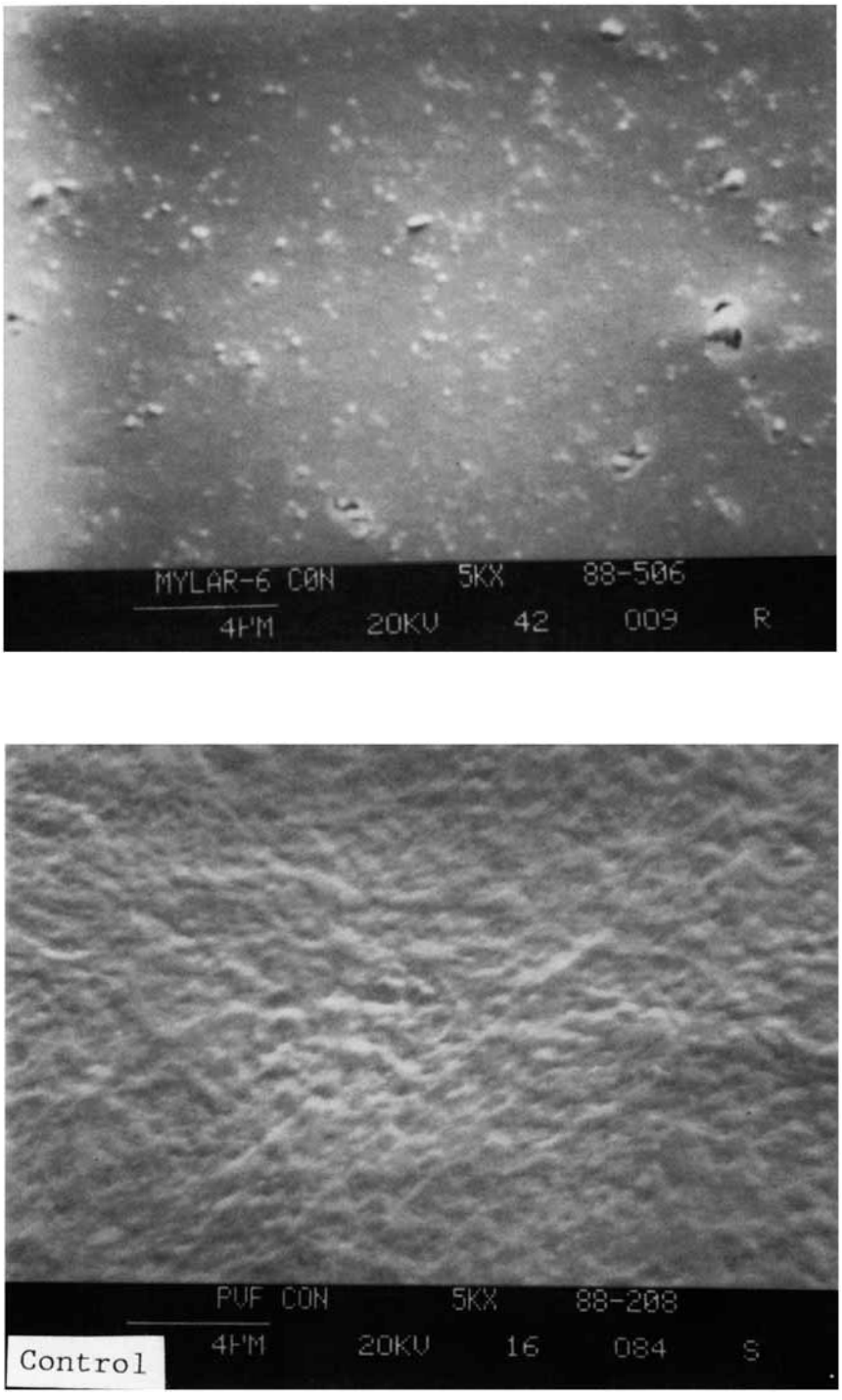


**Figure 17** Atomic oxygen exposed (top) and control (bottom) PVF.

lower pressure, higher energy atomic oxygen, varying material temperature, and longer exposure times. These factors have been shown to affect the surface morphology produced on ion etched materials.[47] The residual stress condition of a material surface was also a contributor to developed structures.[48]

## Model of Atomic Oxygen Reaction With Polymers

Interpretation of generated data suggested that the atomic oxygen reaction in polymers was a thermally activated, two-step process with AO diffusing into the polymer, then initially reacting more readily with

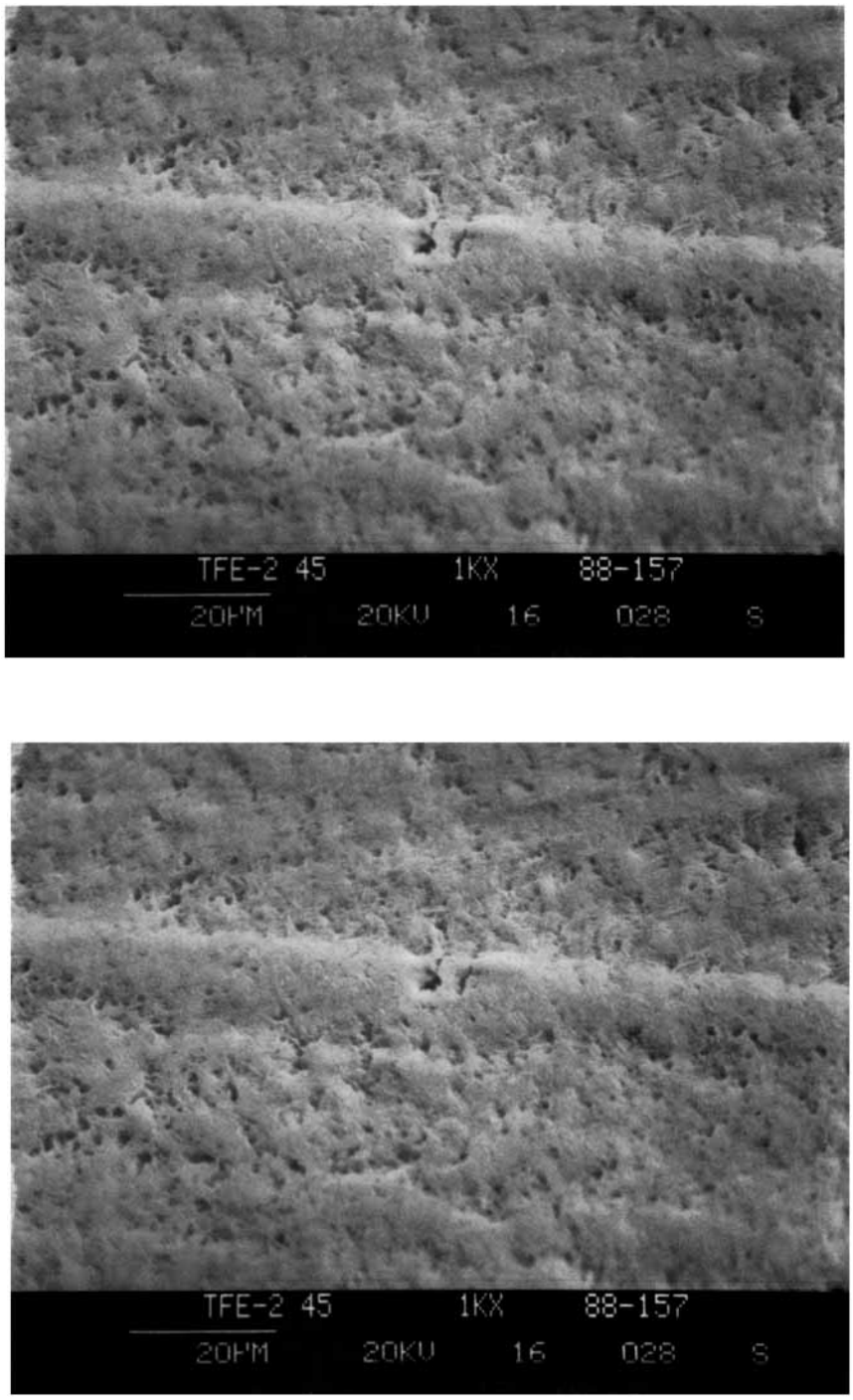


**Figure 18** Atomic oxygen exposed (top) and control (bottom) TFE.

the weaker polymer bonds. Bond strength was a factor in the magnitude of mass loss rate and pendant polymer backbone structures can influence the mass loss rate. Typically for all polymers, out of ten thousand incident atomic oxygen atoms on a 45°C polymer surface, mass loss events accounted for the involvement of 1% or less of these atoms. This suggested a complicated process and implied that reflection and recombinations of AO were occurring, and the involvement of more than one atomic oxygen atom may be assumed in a mass loss event. ESCA and FTIR data suggest that low mol wt gases were formed from these reactions. RGA analyses also supported this data. GPC indicated no reduction in surface mol wt, which implied as the gases escaped the surface, bonds were reformed. Under constant exposure conditions, mass loss was linear in time with the exception of several polymers that tended to form partial or total self-passivating films, such as Mylar and dimethyl silicone. Activation energies were of the magnitude for diffusion in polymers and were consistent with diffusional effects found with polymer increased mol wt and crosslinking. The mass loss rate for atomic oxygen attack can be effectively described by the equation:

$$1/\mathrm{A}\ dm/dt = \delta m/\delta\epsilon \times 1/4n_vV \times \phi e^{-E/RT}$$

## CONCLUSIONS

The following concluding remarks can be drawn from this investigation:

1. The mass loss rate equation for atomic oxygen exposed polymers may be expressed as: $1/A\ dm/dt = \delta m/\delta\epsilon \times 1/4n_vV \times \phi e^{-Ea/RT}$, where the parameters have their previously discussed meanings.
2. Mass loss of polymers under atomic oxygen exposure is a thermally activated process with activation energies in the range of 1 to 48 KJ/mole.
3. The model of polymer reaction to atomic oxygen describes a two-step process of atomic oxygen diffusion into the polymer surface with subsequent reactions with bonds to generate low mol wt gases.
4. The energies of both primary and secondary bonds are an important factor in the reactivity of materials to atomic oxygen.
5. Increased mol wt and crosslinking in polymers retard the atomic oxygen reaction. These factors improve the resistance of polymers to atomic oxygen diffusion.
6. Pendant backbone structures can provide some shielding of the polymer backbone from atomic oxygen attack.
7. The effect of higher energy atomic oxygen impingement on polymer surfaces is to produce more pronounced structures similar to that observed in ion etched surfaces.

This article was based in part on A.F.W.'s PhD dissertation. A.F.W. would like to express thanks to Joey Norwood and David Esker for operation of the Plasmod and to Ed White and Bobby Cothren for maintaining the operation of the test systems. B.Z.J. would like to express thanks for the support of the Alabama Research Institute and National Science Foundation (Materials Engineering and Tribology Program).

## REFERENCES

1. A. F. Whitaker, *The Effects of Atomic Oxygen on Polymer in a Radio Frequency Plasma,* Ph.D. Dissertation, Auburn University, Alabama, March 1989.
2. D. T. Clark and A. Dilks, *J. Polym. Sci. Polym. Chem.* Ed., **17,** 957–976 (1979).
3. J. R. Hall, *J. Appl. Polym. Sci.,* **16,** 1465–1477 (1972).
4. H. Schonhorn and R. H. Hausen, *J. Appl. Polym. Sci.,* **11,** 1461–1474 (1967).
5. M. Stradal and D. A. I. Goring, *Canad. J. Chem. Eng.,* **53,** 427–430 (1975).
6. A. Bradley and J. D. Fales, *Chem. Tech.,* 232–237 (1971).
7. J. R. Hall, C. A. L. Westerdahl, A. T. Devine, and M. J. Bodnar, *J. Appl. Polym. Sci.,* **13,** 2085–2096 (1969).
8. H. Yasuda, C. E. Lanage, and K. Sakaouku, *J. Appl. Polym. Sci.,* **17,** 137–152 (1973).
9. R. Klein and M. D. Scheer, *J. Phys. Chem.,* **72,** 616–622 (1968).
10. K. Rossmann, *J. Polym. Sci.,* **XIX,** 141–144 (1956).
11. R. H. Hansen, J. V. Pascale, T. DeBenedictis, and P. M. Rentzepis, *J. Polym. Sci. Part A,* **3,** 2205–2214 (1965).
12. K. Barabas, M. Iring, T. Kelen, and F. Ludos, *J. Polym. Sci. Symp.,* **57,** 65–71 (1976).
13. F. M. Rugg, J. J. Smith, and R. C. Bacon, *J. Polym. Sci.,* **XIII,** 537–547 (1954).
14. J. R. MacCallum and C. T. Rankin, *Die Makromolek. Chemie,* **175,** 2477–2482 (1974).
15. G. N. Taylor and T. M. Wolf, *Polym. Eng. Sci.,* **20,** 1087–1092 (1980).
16. B. Banks, NASA Lewis Research Center, Cleveland, Ohio, private communication.
17. F. Watanabe and Y. Ohnishi, *J. Vac. Sci. Techn.,* **B4,** 422–425 (1986).
18. S. J. Moss, A. M. Jolly, and B. J. Tighe, *Plasma Chem. Plasma Proc.,* **6,** 401–416 (1986).
19. L. P. Torre and H. G. Pippin, *Structure-Property Re-*

*lationships in Polymer Resistance to Atomic Oxygen,* SAMPE International Conference, Seattle, Washington, Oct. 1986.
20. G. S. Arnold and D. R. Peplinski, Aerospace Report No. ATR-84 (8540).
21. A. F. Whitaker, *RF Oxygen Plasma Effects On Polymeric Materials,* Ph.D. Dissertation, Auburn University, Alabama, March 1989.
22. R. T. Morrison and R. N. Boyd, *Organic Chemistry,* Allyn and Bacon, Boston, 1983, pp. 20–21.
23. J. A. Brydson, *Plastic Materials,* 2nd ed., Van Nostrard Reinhold, New York, 1970, pp. 303–348.
24. R. E. Huie and J. T. Herron, in *Progress in Reaction Kinetics,* Vol. 8, K. R. Jennings and R. B. Cundall, Eds., Pergamon, New York, 1978, pp. 1–80.
25. R. J. Donovan and H. M. Gillespie, in *Reaction Kinetics,* Vol. 1, P. G. Ashmore, Ed., The Chemical Society, Burlington House, London, 1975, pp. 49–70.
26. N. M. Emanuel and A. L. Buchachenko, *Chemical Physics of Polymer Degradation and Stabilization,* VNU Science, Utrecht, The Netherlands, 1987.
27. J. Crank and C. S. Park, *Diffusion in Polymers,* Academic, New York, 1968, pp. 46–50.
28. H. J. Huddy, *Plastica,* **20,** 348–357 (1967).
29. R. A. Pastenak, M. V. Christensen, and J. Heller, *Macromolecules,* **3,** 366–371 (1970).
30. W. J. Kores, J. Wang, and R. M. Felder, *J. Appl. Polym. Sci.,* **26,** 2805–2809 (1981).
31. R. T. Saunderson, *Chemical Bonds and Bond Energy,* 2nd ed., Academic, New York, 1976, p. 19.
32. D. W. Van Krevelen, *Properties of Polymers Their Estimation and Correlation with Chemical Structure,* Elsevier, Amsterdam, The Netherlands, 1976, pp. 411–415.
33. J. Crank and G. S. Park, *Diffusion in Polymers,* Academic, New York, 1968, pp. 107–136.
34. K. D. Ziegel and F. R. Eirich, *J. Polym. Sci. Part A-2,* **8,** 2015–2027 (1970).
35. P. B. Macedo and T. A. Litovity, *J. Chem. Phys.,* **42,** 245–256 (1965).
36. B. Meissner, *J. Polym. Sci. Polym. Lett. Ed.,* **19,** 137–142 (1981).
37. S. M. Aharoni, *J. Macromol. Sci. Phys.,* **B9,** 699–731 (1974).
38. S. M. Aharoni, *J. Appl. Polym. Sci.,* **23,** 223–228 (1979).
39. G. P. Koo, *Fluoropolymers,* L. A. Wall, Ed., Wiley–Interscience, New York, 1972, p. 515.
40. S. M. Aharoni, *J. Macromol. Sci. Phys.,* **B9,** 700–701 (1974).
41. W. Schnabel, in *Aspects of Degradation and Stabilization of Polymers,* H. H. G. Jellinek, Ed., Elsevier, New York, 1978, pp. 149–158.
42. L. J. Bellamy, *The Infra-Red Spectra of Complex Molecules,* Wiley, New York, 1958, pp. 13–60.
43. V. Stannett, *Diffusion in Polymers,* J. Clark and G. S. Park, Eds., Academic, New York, 1968, p. 68.
44. J. A. Brydson, *Plastic Materials,* 4th Ed., Butterworth, Boston, 1985, p. 512.
45. MSFC Data Report 91-3-24-88.
46. F. D. Egitto, F. Emmi, and R. S. Harwoth, *J. Vac. Sci. Technol.,* **B3,** 893–904 (1985).
47. G. Turban and Michel Rapeaux, *J. Electrochem. Soc.,* 1983, pp. 2231–2236.
48. R. H. Liang, A. Gupta, S. Y. Chung, and K. L. Oda, *Mechanistic Studies of Polymeric Samples Exposed Aboard STS VIII,* JPL Publication 87–25, December 15, 1987.

*Received July 19, 1991*
*Accepted August 11, 1992*